HALMSTAD UNIVERSITY

Master's Programme (60 credits) in Renewable Energy Systems

MASTER THESIS

Fault Location Algorithms in Transmission Grids

Mattias Harrysson, Energy Engineer - Renewable Energy

Dissertation in Engineering Energy

Halmstad 2014-06-02

Acknowledgements

This thesis was carried out in the Master's program in Energy science during the spring of 2014. It was done in collaboration with Enfo Energy and the Norwegian transmission system operator Statnett.

I would like to thank the whole team at Enfo and the research development at Statnett for giving me the opportunity to work on this research.

I want to express my gratitude to Prof. Jonny Hylander for the freedom he gave me and the trust he put on me during my master period. I am also grateful to Dr. Eilert Bjerkan for his support and advice, especially for reorienting the topic of the thesis at the right time. His high level view of power systems and smart grid truly contributed to this document.

I would like to thank all the colleagues of the department for the interesting discussions and great working atmosphere. Special thanks also to Pål Vidar Strømmen for the technical discussions and review of this document and Bernt Sørby for his expertise in programming of the model.

Finally, I wish to thank my family and friends for their unwavering support.

Abstract

The rapid growth of the electric power system has in recent decades resulted in an increase of the number of transmission lines and total power outage in Norway. The challenge of a fast growing electrical grid has also resulted in huge increases of overhead lines and their total length. These lines are experiencing faults due to various reasons that cause major disruptions and operating costs of the transmission system operator (TSO). Thus, it's important that the location of faults is either known or can be estimated with reasonably high accuracy. This allows the grid owner to save money and time for inspection and repair, as well as to provide a better service due to the possibility of faster restoration of power supply and avoiding blackouts.

Fault detection and classification on transmission lines are important tasks in order to protect the electrical power system. In recent years, the power system has become more complicated under competitive and deregulated environments and a fast fault location technique is needed to maintain security and supply in the grid.

This thesis compares and evaluates different methods for classification of fault type and calculation of conventional one-side and two-side based fault location algorithms for distance to fault estimation. Different algorithm has been implemented, tested and verified to create a greater understanding of determinants facts that affect distance to faults algorithm's accuracy. Implemented algorithm has been tested on the data generated from a number of simulations in Simulink for a verification process in implemented algorithms accuracy. Two types of fault cases have also been simulated and compared for known distance to fault estimation.

Table of contents

Introduction

The need for accurate fault location techniques in the transmission grid is increasingly becoming more important. The electric power system is expanding in size and complexity and will always be exposed to failures and storms. The Norwegian transmission system operator (TSO) Statnett has started a substantial investment in the national grid. Several hundred kilometers will be built or upgraded each year to meet the society's rapid growing need for capacity powered highways. So, when a fault occurs on a transmission line, it's very important for the TSO to identify the fault location as quickly as possible to improve and maintain a sufficient reliability.

Perspectives

The rapid growth of the electric power system has in recent decades resulted in an increase of the number of transmission lines and total power outage in Norway [11] . Also, introduction of greater intermittent sources have resulted in more restrictive requirements in order to provide a continuous good quality of delivered electricity, without any major impact on the energy delivered cost. Uninterruptible power supplies, security and reliability aim an important role in the future power system; as a result of imposing restrictive requirements, the transmission system will handle these challenges smarter to secure safe power delivery in known energy market. The consumers are more sensitive to power cuts and electricity frequent intermittent disruptions in today´s modern society. A smart solution is required to identify problems in the grid reliably and quickly and without any operational disruptions. A smarter transmission grid with new smart grid components, communication and operational control, may solve parts of this challenge.

The challenges of a fast growing electrical grid has also resulted in huge increases of overhead lines and their total length, these lines are experiencing faults due to various reasons that cause major disruptions and operating cost of the transmission system operator (TSO). The transmission system experience disruptions caused by storms, thunder, snow, freezing rain, insulation breakdown and short circuits caused by birds and other external objects [B.1.]. In majority, faults are caused by mechanical and terminal failure, which must be repaired before the transmission lines are operational again. Intermittent faults are self-cleared and do not affect the power supply permanently. A fault location of such fault is important and can help to find or pinpoint a weak spot on the line. As a result, the maintenance schedules can be fixed, avoiding further disruptions in the future. Temporary failure or a major disruption will not only create problems in power electronics and components, but also create a large economic penalty cost for the grid owner. Thus, it's important that the location of faults is either known or can be estimated with reasonably high accuracy. This allows the grid owner to save money and time for inspection and repair, as well as to provide a better service due to the possibility of faster restoration of power supply and avoiding blackouts [B.1.][B.2.].

Therefore, fast detection, isolation, location and repair of such faults are an important role in order to maintain the power system in a healthy condition.

Fault location today known by regular fault locator based on microprocessor- protective relay, digital fault recorder (DFRs) or stand-alone fault locators. A fault locator is mainly the supplementary protection equipment, which apply the fault location algorithm for estimation distance to fault [B.2.]. Depending on the type of signals that the fault locator use, the fault location methods can be further classified into different categories. Impedance based fault location algorithms, generally classified as one-terminal methods and two terminal methods (synchronized or unsynchronized data from both terminals). Other fault location methods use travelling waves to consider current and voltages waves with high sampling frequency. Travelling waves methods are considered very accurate and at the same time very complex and high in cost of implementation.

Objectives and approach

This thesis compares and evaluates different methods for classification of fault type and calculation of distance to fault. The purpose of this thesis is to examine the applications of conventional one-side and two-side based fault location methods for transmission grid overhead lines. Different type of algorithm will be verified in Simulink and be implemented to the transmission line analyses of different known fault cases. The project will be divided into different work packages with main focus on implementation, verification, testing and benchmarking of algorithms for calculating the distance to fault:

- Literature research to identify state-of-art methods for calculating the distance to fault in different fault type's scenario.
    - Research in relevant literature in relay protection, fault analysis, fault location algorithm and fundamental information about fault sequences in the transmission grid.
- Implementation of selected algorithms in MATLAB and Simulink for verification of distance to fault and fault location methods weakness and accuracy in different fault cases.
    - Suggest test case verification of five selected one-side algorithm and four two-side algorithms.
    - Develop sequencer and visualization tools for determine fault type with valid test methods.
    - Create an understanding of selected algorithms in fault location analysis.
- Suggested two test cases with valid data from the transmission lines fault recorder with calculated distance to fault.
    - Fault case (weather conditions), one fault cases with permanent faults with known repair-location, fault case (one-phase fault, two-phases fault, three-phase fault will be evaluated for the different methods)
    - Calculated result from MATLAB will be presented and compared for different fault location methods statistically in order to create a reliable result from the algorithms strengths and weaknesses at different fault cases.

- Compare, calculated and simulated results with valid data and information from the transmission lines fault.
- ***If there is time***: Evaluate theoretical tools and general information source that will provide a better understanding and knowledge about fault location methods and distance to fault.
    - Where performed calculations and information from test cases be compared with metrological characteristics; Lightning (geographical point of impact), wind (direction) and temperature (icing, humidity).

Contribution

The main contribution of the thesis is two methods, methods 1 and 2 for implementation of distance to fault algorithm and estimation and value distance to fault cases in the Norwegian transmission grid. The methods are based on conventional distance to fault localization algorithm, and the algorithm is implemented in MATLAB R2014a Simulink for verification. Data and information from transmission line and load are basically obtained from fault recorder and phasor measurement units (PMU). Distance to fault calculation using conventional one-side and two-side based fault localization have been investigated.

Method one estimates and verifies algorithms' accuracy in a structured and programmed Simulink model. Five one-side and three two-side algorithms with different applications have been presented and calculated.

Method two utilizes measurement from the Norwegian transmission system during which specific fault have been tested and analyzed with the developed distance to fault model. The method thus requires measurement from the transmission network during fault. The input data during specific fault situation fault are estimated and calculated from developed MATLAB model. The distance to fault algorithm needs information about phasor angle, true RMS-value and synchronization time measured between values from both substation side at fault and pre-fault.

A method of finding correct data and inputs have been developed before and the new methods for distance to fault estimation are implemented in Statnett's R&D program Autodig.

Organization of thesis

The thesis is divided into eight chapters and three additional appendix chapters. Short descriptions of each chapter are given here.

Chapter one puts the work of this thesis into context of fundamental background of transmissions lines configuration for fault location.

Chapter two explains fault reasons and statistics on transmission grid in Norway. The chapter also explains different fault types and fundamental information about fault detection and localization.

Chapter three describes and explains different fault location methods of one-side and two side fault location algorithms structure and functionality. Five one-side and two two-side algorithms is presented and the methodology and mathematics of each algorithm are discussed and presented.

Chapter four describes the research methodology behind the verification process of MATLAB R2014a, and the Simulink methodology profile and input value. The chapter also presents verification results of all algorithms in Simulink. Table and plots of the distance estimate errors for various cases shown.

Chapter five presents results of the three test cases with valid data from the transmission lines fault recorder with known distance to fault. Calculated results from MATLAB R2014a are presented for the selected test cases with the different fault location methods.

Chapter six contains discussion about the verification modelling and the result.

Chapter seven contains conclusions.

Appendix A-C is to be found at the end of the thesis.

Statnett

Statnett is the system operator in the Norwegian energy system. This means operating about 11 000 km of high-voltage power lines and 150 stations all over Norway. Operations are monitored by one national control center and three regional centers. Statnett is also responsible for the connections to Sweden, Finland, Russia, Denmark and the Netherlands.

Statnett has given me access to resources and power system engineers from the Fault Analysis Department during the research phases of my Thesis. Historical data related to grid disturbances are also part of Statnett contribution and used extensively throughout my research.

Fault statistics

Nordel comprises statistics of fault through the Nordic organization and comprises fault and power system disturbance in each Nordic country. Previous studies of the Norwegian fault statistics have shown that the protection system has a large number of uncorrected operations, this is a significant contributor to energy no supply (ENS) and thereby the customers interruption's cost [11] The transmission system operator has in the last year increased the focus on reliability and security of supply. This is because a growing market of delivered power where the system is operated closer to the limit.

The number of faults in Norway is the second highest rate in Scandinavia; these can be explained by geographical and structural differences [11] .The Norwegian grid between the northern and southern part is quite weak because of the long and narrow country with a long coastline, many fjords and mountains. The transmission system consists of 420, 300, 220 and 132 kV overhead lines and cables and average line fault frequencies are considerably 400 kV faults, natural causes (lighting, wind etc.). Meteorological causes count for more than 35 % of the disturbances and more than 30 % of ENS (energy not supply). The large cause of ENS in Norway has technical aspects and a third of all fault causes by the fault in protection and control system. Operation, maintenance and technical failure dominate human causes and together the fault rate is 50 % of the unwanted trips [41] .

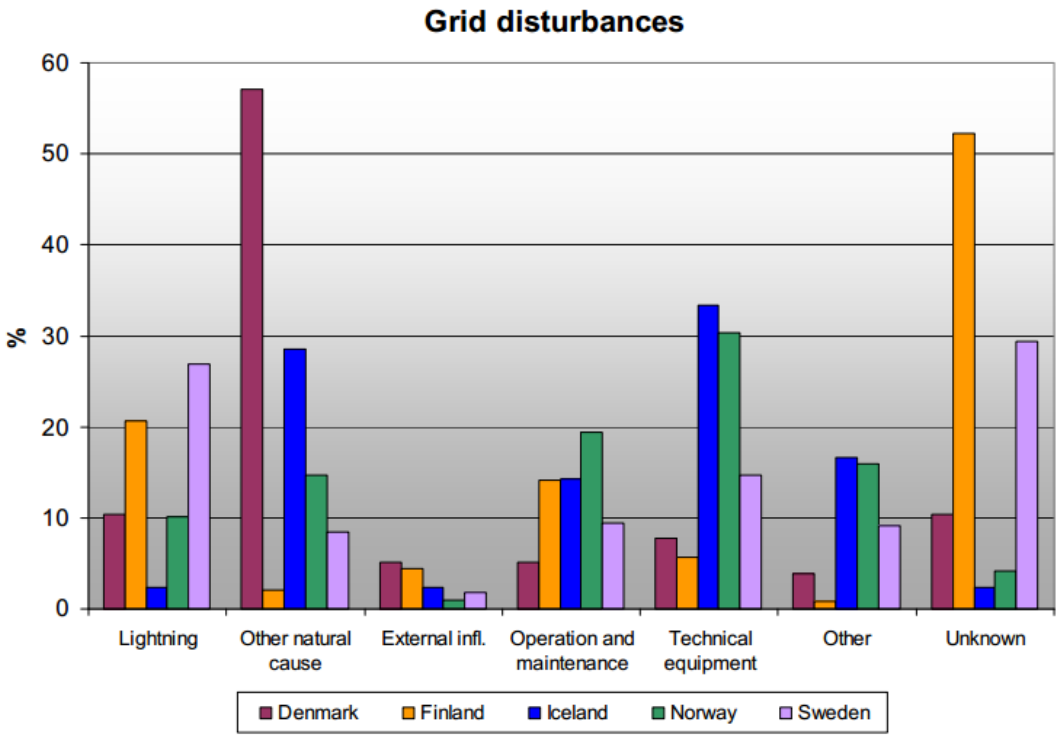

Figure 1: Grid disturbances divided according to cause in 2007 [41]

Chapter one

Method

This project was created in collaboration with Enfo Consulting AS and Statnett. The background of the project was discussed during the autumn of 2013. The objectives of the project were presented in introduction of this thesis.

The structure of the thesis was discussed with the mentor during scheduled appointments. The project is mainly a literature review about fault location algorithms for the transmission grid. The working process of this thesis has mostly involved compilation and evaluation of the gathering information, the writer has also implemented and verified the chosen algorithms in MATLAB R2014a and Simulink.

Five one-side algorithms and three two-side algorithms were studied and implemented in the project. A simulation model was developed in Simulink for verification of the algorithms accuracy at different fault cases. Three known fault cases in the Norwegian transmission system were then evaluated and analyzed for each fault cases with a developed model for distance to fault calculation.

Sources of information

The library at Halmstad University helped with searching information in various databases; the information comes from scientific articles found in the database, course literature and books. Statnett and Enfo contributed with data and programming reconstruction of the distance to fault application, as well as important information and knowledge from colleagues and employees of Statnett.

Chapter two

Transmission Line Fault

This chapter presents the basics of transmission system line faults. Transmission system line faults are the most common faults, triggered by falling trees, lighting strikes or insulator string flashover and 85-87% of power system faults are occuring in the transmission lines [41] . Most of the transmission system faults occurs on overhead lines, due to their inherent characteristics of being exposed to atmospheric conditions [15] . Faults occur in the power system of various causes. For example, lightning strike can overload the system's components and result in a breakdown of the insulation in overhead lines. The impedance of source connections are often very low, resulting in large currents flowing during faults . The energy contained in a fault current can quickly create excessive heating or forces to components and can result in devasting explosions of equipment. Short-circuit causes, over short interuptions with voltage dips damage the grid and creating major disturbances and cost. Faults occur in many different forms depending of the fault type and the algorithm for calculating distance to fault will therefore vary. Faults on transmission overhead lines are in majority temporary single phase to ground, arcing faults [12]

Fault Types

A power system fault can either be shunted, series or combination of both type, shunt fault providing a current flow between two or more phases, or to earth. Shunt faults occurs through a breakdown of insulation betweend the phases, or earth. Shunt faults often occur in two different ways; abrupt changes of the lines voltage and current characteristic, due to lighting strike, birds, threes or simular; or slowly deterioration of the lines insulation.

Slow deterioration of insulation will gradually create poor components and worn material that will age over time. Sometimes the difference between slow changes and abrupt faults is not strictly clear. It's possible to talk about faults that occur suddenly, but have evolved over longer period of time. Failure like this is typical faults that are caused by phases to phase merging, due to snow, icy lines or strong wind[B.1.][B.2.][B.3.] . When a fault occurs, the fault current will increase in magnitude, the total amplitude of fault current during a fault depends upon a variety of factors, such as fault type, network, fault resistance, failure causes load currents, short circuit levels etc. Typical shunt faults are presented below:

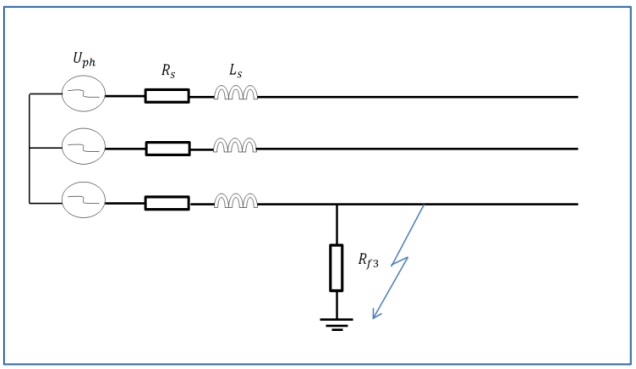

Figure 2 : line-to-ground fault (L-G)

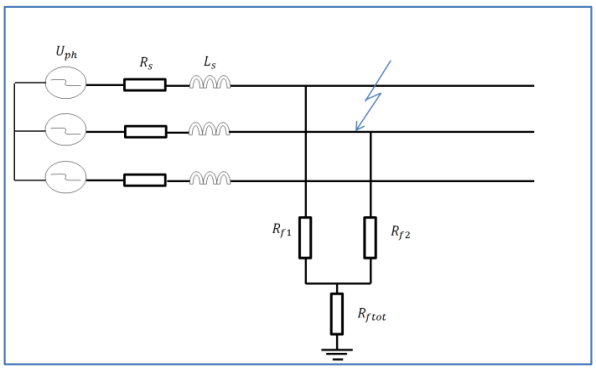

Figure 3: Line-to-line to ground fault (L-L-G)

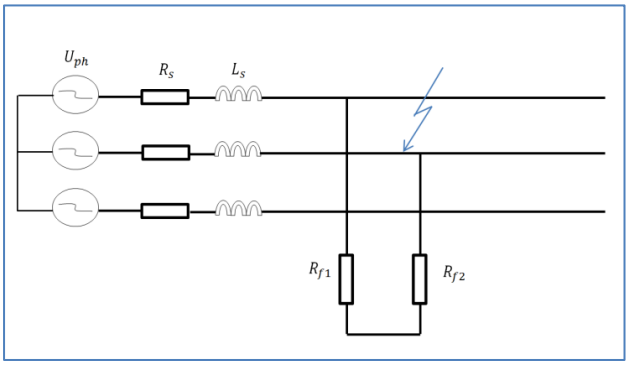

Figure 4: Line-to-line fault (L-L)

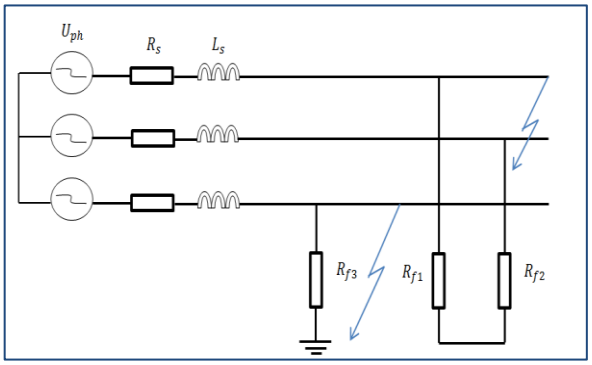

Figure 5: Line-to-line fault and line-to-ground fault (L-L,L-G)

Fault in which the balanced state of the network are called unsymmetrical or unbalanced faults. The most common faults are single-to-line to ground faults line-to-line faults and double-line-to-line faults. All of these are unbalanced fault or asymmetric fault.

Common fault on an transmission line [43][42]

- Line-to-line fault – short circuit between lines caused by phisical contact between two lines 60-75 % of all fault in the system line-to-line faults (For example, broken conductor or strong wind).

- Line-to-ground fault – short circuit between one phase and ground caused by physical contact, 15-25 % are line-to-ground fault (Ex. lightning and external factors).

- Line-to-line-to ground fault – short circuit of two line and ground, and 5-15 % are line line-to-line to ground faults. (Ex. external factors)

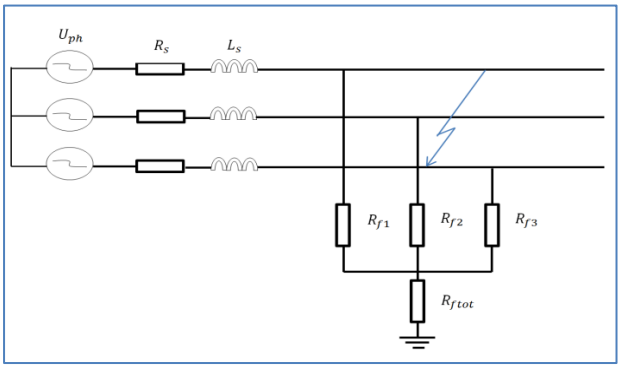

Figure 6 : line-to-line-to-line to ground fault (L-L-L)

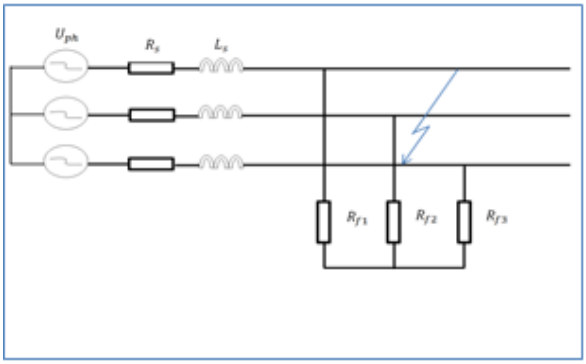

Figure 7: : line-to-line-to-line fault (L-L-L-G)

A three phase symmetrical fault is caused by application of three equal impedances to the three phases, as shown in *(Figure 6).* Balanced faults are categorized in two fault types called solid or a bolted fault. These faults can be of two types: Line-to-line-to-line ground fault or without ground. Since all the three phases are affected, the system remains balanced. A balanced fault in the transmission system is very uncommon and only 5 % of the system fault is three phases fault [B.1.][B.2.][B.3.] [B.4.].

Broken conductor fault

Other faults like broken conductor faults are series faults which involve a break in one or two of the three conductors of a three phase power system. In this case, the fault is an unsymmetrical series fault and thus, the theory of symmetrical components was revisited [26] . A series fault is an abnormal condition, since the impedance in the three phases is not equal [6]

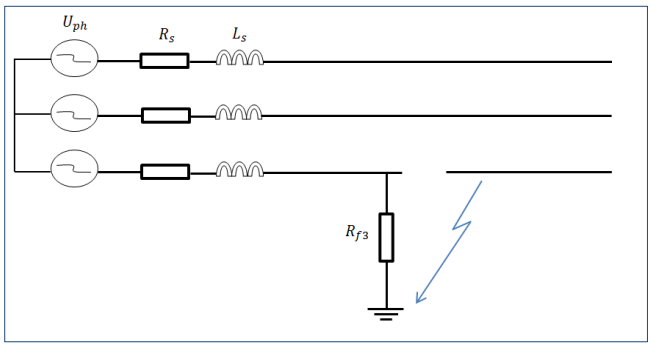

Figure 8 : Broken conductor and line-to-ground fault.

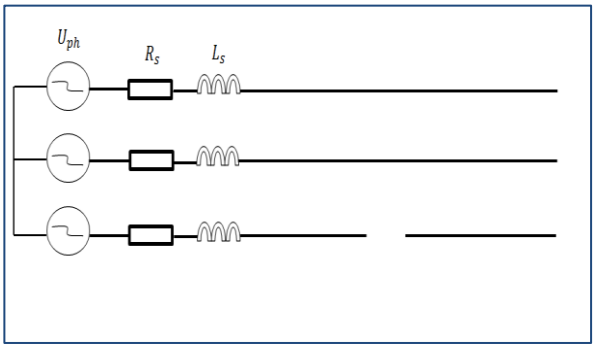

Figur 9: Broken conductor.

When one or two phases of a balanced overhead three-phase line open it creates unbalance in the system and may result in high unbalanced currents and voltages. Such condition usually occurs when the conductor of a transmission line is broken or damaged. Broken conductor faults are usually caused by variable weather condition and climate influences to the power grid.

Conductor icing is a comprehensive physical phenomena determined by meteorically factors, temperature fluctuation, humidity, wind and other weather factors. A known physical phenomenon in when cold weather accumulate ice on the conductor, and when the ice suddenly drops the dynamic effect of the transmission line will cause major electrical and mechanical failure. Electrical failure between adjacent conductors and the ground lead to flashover or electrical shock. From a mechanical view, high amplitude vibrations may break one conductor or more and this will result in large unbalance in the phases [9] .

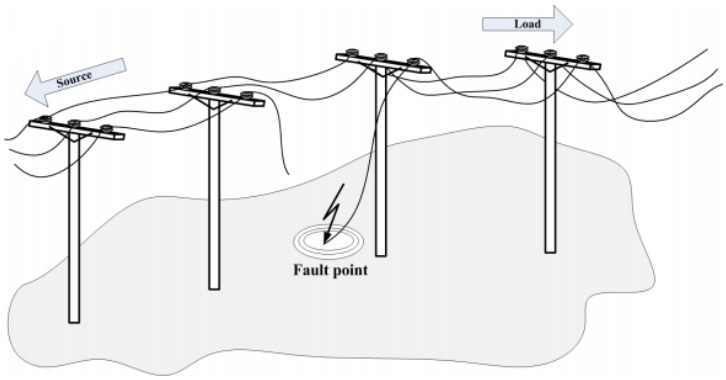

Figure 10: Down Conductor fault on overhead line [4]

Strong wind may also create aeolic harmonics vibration on power transmission lines; these vibrations are associated with great tension on the conductors, which can lead to broken conductors. This phenomenon, where the conductors come in contact with one another during strong wind or other external forces, is called conductor clashing [10] .

Arcing Faults

At a high voltage flashover in voltage magnitude, an arcing fault may occur and cause fault situation on the transmission grid. An arcing fault can be considered as a current dependent resistance with three zones. Area closes the adjacent points can be described as a voltage drop independent of current magnitude, arc is spreading if there is space available [5] If the flowing current through the arc is high the arcing fault through ionization becomes more powerful and the resistance lower. The fault resistance is much larger in the main part of the arc than in the end points

An electrical arc is affected by magnetic forces and wind, but also the heat extension during the development of an electrical arc. Because of this, its length will increase over time, and if the condition is right the arc may escalate through the conductors and cause short circuits. In the initial phase of an arc fault the arc's length will be extended, and so over until a disconnection occur. Flashover and arc faults on overhead lines caused by power surges (e.g. lightning) usually occur over the isolators because the arc distance is shortest at these points [5] .

In a short circuit causes the acing resistance is very low compared to the impedances, especially during the fault measurement time of a protective. To calculate the maximum fault current the acing resistance sets to zero. This is because a nonlinear arc resistance causes a certain harmonic content in the fault current that protective relay must accept.

External Faults

Lightning faults and faults caused by trees are the most common faults on overhead lines. In the transmission grid lightning faults are dominate because the overhead line here are more tree secured. Losses in overhead lines are resistive and the created losses can be seen as a series resistance at the overhead lines' end points. Current flow in overhead line creates a magnetic field around the conductor in overhead lines is this called line reactance. Reactance between the conductor's phases and to ground creates an electrical field; this can be seen as a capacitance. Lightning's fault usually appears when lightning strikes a phase conductor directly, but there are also other places where a lightning strike can create a fault, depending of the size of earth resistance and lightning's voltage amplitude.

When a lighting fault occurs on an overhead line an arcing will occur over insulators, phases and insulator bracket. If the isolator bracket is connected to ground, a ground fault has occurred. Ground fault can be either single-phase or multiphase fault, depending how many phases involved. Ground fault voltages into a properly grounded network have low value for cases where all three phases are involved; if the ground fault voltage phase voltage reaches a high level earth fault has occurred.

Lighting strike on 400 kV network is virtually all single-phase fault, if there are two or more phases inductor on the grid the lighting strike usually occurs on all phases at same time. If the voltage is moderate and the insulation strength is higher than normal voltage level, an individual conductor may have been involved. Besides lightning strikes, other types of fault can occur on overhead lines in the transmission system. These external faults may include phase failure, defective insulators or failure due to snow and ice, salt or other contamination.

Fault detection

Fault detection and classification on transmission lines are an important task in order to protect the electrical power system. In recent years, the power system has become more complicated under competitive and deregulated environments. Protection relay classifies the fault type and also classifies the "normal state" of the power system. The abnormal condition of the power grid is detected by information in the phase's impedance, current, voltage and the zero-sequence current amplitude. Together with many other applications as breaker position, monitoring of power flow on line etc. [B.1.]. The traditional algorithm for fault detection and classification, which is mostly based on steady-state components, has problems to handle the accelerating protection speed and in escaping the impact of many factors, such as fault type, fault resistance and inception time. Different fault detection algorithms are presented in chapter five.

Reliable phase selection of faulted phase is important to avoiding tripping phase or unnecessary three-phase tripping [18] Classification and fault detection is not an easy task. Different types for fault classification have been presented the last decades. Some of these are based on traveling waves, adaptive filtering and the fusion of different artificial intelligence techniques [18] . The most simple fault determination methods assume that phase impedance during fault can be correlated with the maximum load. In addition, the zero-sequence current is used as an indicator of fault with ground fault.

Another method uses the superimposed current of pre-fault and fault to classified fault. A more common method is the use of symmetrical components of fault current and voltages. These methods obtain a reliable decision and important information about the phase angle[1].

[1] Fundamental information about symmetrical components in Appendix A

Chapter three

Fault Location Methods

In this chapter, different types of fault location algorithms are presented. The most common fault location algorithm principles are based on impedance-based methods. One-ended impedance based fault location algorithm estimate distance to fault with the use of voltages and current at a particular end of the line. The technique is very simple and does not require any communication with the remote end [24] .The algorithms presented in this chapter are designed for location of fault on single lines, double lines and series compensated lines. The one-ended fault-location algorithms are very simple and economical, compared to two-end methods.

One-Ended fault location algorithm

The majority of one-end fault-location algorithm is based on calculation of fault loop composed to identify fault type, similar to the distance relay [B.1.][B.2.]. One-ended impedance methods of fault location are a standard feature in most numerical relays. The methods use a simple algorithm, communication channel and remote data are not required. The impact of fault resistance on one-end impedance measurement is a key factor in deriving the majority of one-end fault-location algorithm. Fault locators calculate the fault location from the apparent impedance seen by looking from one end of the line [3] Fault types usually coincide by the phase to ground voltages and current in each phase, it is also possible to locate phase to phase faults by the zero-sequence impedance (Z_{L0}).

The majority of all one-ended fault location is based on a "fault loop" composite for identified the fault type. The following formulas calculate the apparent impedance from the feeding busbar (S) for distance relays [B.1.][2] [6] .

$$Z_s = \frac{V_s}{I_s} \qquad \textit{Eq 1}$$

Fault calculation is laid down by the fault impedance with compensation for fault resistance drop. For determined fault where fault resistance $(\mathrm{R_f} = 0)$ is the apparent impedance equal to the positive sequence impedance$(\mathrm{Z_{L1}})$ of the line segment by distance (m) from the measuring point until the fault according (*Eq 2*).

$$Z_s = m * Z_{L1} \qquad \textit{Eq 3}$$

If not taken account to the positive sequence line impedance at resistive fault, the calculation will probable estimate wrong distance to fault.

The other important aspect of this fault locator algorithm is the use of the pre-fault current in order to establish the variation of line current at fault. The first equation will return here as positive-sequence impedance equation (Eq 21*)*. A voltage is the sum of the drop in the line to the fault point.

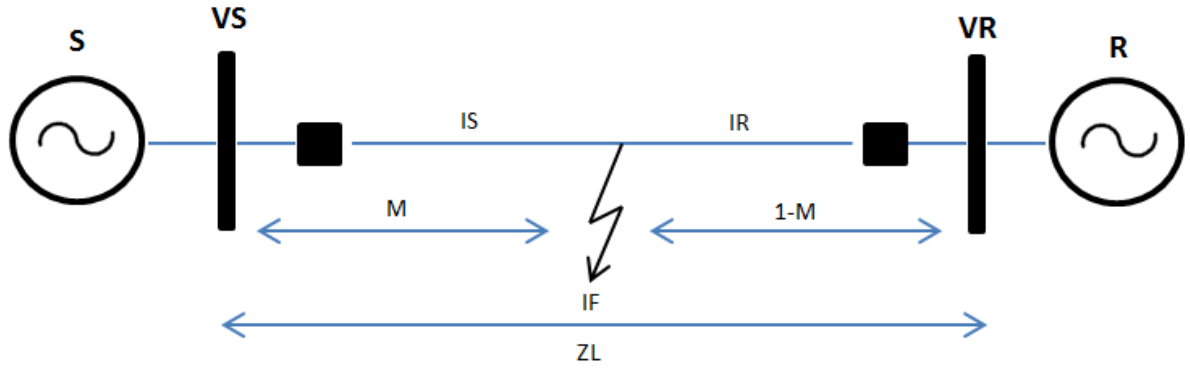

Figure 11: Single transmission line model

$$V_s = m * Z_{L1} * I_s * R_f * I_f \qquad Eq\ 4$$

Where:

$V_s = voltage$

$I_s = current$

$I_f = current\ at\ fault$

$Z_{L1} = positive - sequence\ \ line\ impedance\ nominal\ value *$

$R_f = resistance\ at\ fault$

$m = per\ unit\ distance\ to\ fault$

Single line (positive-sequence impedance equation)		
Fault type	Fault loop voltage: V_{sp}	Fault loop current: I_{sp}
A-ground	V_{sa}	$I_{sa} + k * I_0$
B-ground	V_{sb}	$I_{sb} + k * I_0$
C-ground	V_{sc}	$I_{sc} + k * I_0$
a-b or a-b-g	$V_{sa} - V_{sb}$	$I_{sa} - I_{sb}$
b-c or b-c-g	$V_{sb} - V_{sc}$	$I_{sb} - I_{sc}$
c-a or c-a-g	$V_{sc} - V_{sa}$	$I_{sc} - I_{sa}$
a-b-c	$V_{sa} - V_{sb}, V_{sb} - V_{sc}, V_{sc} - V_{sa}$	$I_{sa} - I_{sb}, I_{sb} - I_{sc}, I_{sc} - I_{sa}$

Table 1 : Standard calculation on single line with positive-sequence impedance methods equation

For a fault between two phases, the impedance can be obtained from the substations voltage and current in the involved phases. The difference between the two-phase voltages is divided by the difference between phases current. For a three-phase short circuit the voltage and current in any pair of phases can be used for distance to fault calculation.

Reactance Based Algorithm

Novosel simple reactance method, algorithms reported in [B.1.][B.2.][14] [35] [36] extend simple reactance method by making assumptions to eliminate effect of remote infeed and fault resistance. One-ended impedance methods of fault location are standard feature in most numerical relay. The reactance fault location algorithms depend on accurate values of the positive $(\mathrm{Z_{L1}})$ and zero –sequence impedance $(\mathrm{Z_{L0}})$ to determine locations of faults on the transmission line. The positive – and zero-sequence impedance of the transmission line can be verified when a fault location relay is installed at each end of the transmission line. The positive-sequence impedance has verified that it can be used to check the values of the zero-sequence impedance of the line as used by each relay [14] . The method also uses the value of voltage drop from one side busbar of the line, and the value of current depend of type of fault and symmetrical components. Transmission line impedance (Z) is typically dominated by the reactive components (X) and the fault impedance is typically dominated by the resistive components (R).

$$V_s = m * Z_{L1} * I_s * R_f * I_f \qquad \textit{Eq 5}$$

The current flowing through $(\mathrm{R_f})$ is the sum of the local source $(\mathrm{I_s})$ and the remote source $(\mathrm{I_R})$.

$$I_f = I_s + I_R \qquad \textit{Eq 6}$$

$$I_s = I + k * 3 * I_0 \qquad \textit{Eq 7}$$

Where:

$I_0 = zero - sequence\ current$

$k = \dfrac{Z_{L0} - Z_{L1}}{3Z_{L0}}$

The simple reactance method divides all terms by $(\mathrm{I_s})$.

$$\frac{V_s}{I_s} = \frac{m * Z_{L1} * I_s}{I_s} + \frac{R_f * I_f}{I_s} \qquad \textit{Eq 8}$$

Imaginary components of each term mitigate the fault resistance.

$$Im\left(\frac{V_s}{I_s}\right) = Im(m * Z_{L1}) + im(\frac{I_f}{I_s} * R_f) \qquad \textit{Eq 9}$$

Both $(\mathrm{I_s})$ and $(\mathrm{I_R})$ have the same angle and the imaginary part of $im(\frac{\mathrm{I_f}}{\mathrm{I_s}} * \mathrm{R_f})$ is zero in a homogenous system.

$$m = \frac{Im\left(\frac{V_s}{I_s}\right)}{Im(Z_{L1})} \qquad \textit{Eq 10}$$

For this equation $(\mathrm{V_s})$ is the phase-to ground voltage for given fault, $(\mathrm{I_s})$ is the compensated phase current for a phases-to-phases faults and equals phase current difference for a phases-to-phases faults. These methods calculate an estimated fault location in the transmission system.

In a non-homogenous system $(\mathrm{I_s})$ and $(\mathrm{I_R})$ will have a different angle and the imaginary part will show up in the fault as an error term.

$$Im\left\{\frac{|\ I_f\ |}{|\ I_s\ |}\angle(\delta - \alpha) * R_f\right\} \qquad \textit{Eq 11}$$

Inducing of the simple reactance method has some drawbacks as impact by load and introduces error in fault resistance in non-homogenous system.

Takagi method

Takagi impedance based algorithm, with uses of pre-fault and fault data [B.1.][14] [25] [34] [35] [36] . Use pre-fault and fault data to reducing the effect of load flow and minimizing the effect of fault resistance.

Fault location algorithm by takagi method calculates the reactance of faulty line using one-terminal voltage and current data of the transmission line. When a fault occurs on a transmission line the data of pre-fault current are stored immediately and the fault phases are selected. The Takagi method introduces superimposed current $(\mathrm{I_{sup}})$ to eliminate the effect of power flow. This method assume constant current load model and require both pre-fault and post –fault data. The key to success of the Takagi method is that the angle of $(\mathrm{I_s})$ is the same as the angle of $(\mathrm{I_f})$. In an ideal homogeneous system, these angles will be identical. As the angle increases, the errors in fault location also increase.

$$Im(\frac{V_s}{I_{sup}^*}) = m * Im\left(Z_{L1} * I_s * I_{sup}^*\right) + Im(R_f * I_f * I_{sup}^*) \qquad \textit{Eq 12}$$

$$I_{sup} = I_f - I_{pre} \qquad \textit{Eq 13}$$

If complex number $(\mathrm{I_f})$ and $(\mathrm{I^*_{sup}})$ have the same angle as $(\mathrm{R_f})$ in a homogenous system will a multiplication of $(\mathrm{I^*_{sup}})$ take the imaginary part of the equation and eliminate $(\mathrm{I_f})$ according (*Eq 14).*

$$m = \frac{Im(V_s * I^*_{sup})}{Im(Z_{L1} * I_s * I^*_{sup})} \qquad \textit{Eq 14}$$

Takagi method, one-terminal fault method, simply assumes that the three sequences network distribution factors are equal can lead to undesirable error because the zero-sequence current $(\mathrm{I_0})$ is not known as reliably as the positive-sequence current $(\mathrm{I_1})$. In reality, the fault current is not uniformly distributed when a ground faults occurs [15] . Takagi methods can be improved by applying the 3/2 factor in deriving superposition current to compensated for the removal unreliable zero-sequence current [30] .

$$I_{sup} = (3/2)(I_f - I_{pre}) \qquad \textit{Eq 15}$$

Modified takagi method

Modified takagi method eliminates the need for pre-fault data and uses the zero sequence current $(\mathrm{I_0})$ term or negative sequence current (I_2) for ground faults [14] [B.1.].

The zero-sequence Takagi method, which is suitable for single-phase-to-ground faults, has an advantage that does not require pre-fault current measurements. The expression for this algorithm is:

$$m = \frac{Im(V_s * 3I^*_0)}{Im(Z_{L1} * I_s * 3I^*_0)} \qquad \textit{Eq 16}$$

The algorithm is developed with the assumption that the zero sequence system is homogeneous. If this assumption is not fulfilled, the fault location become very sensitive to an angle difference between S and R side and the method can be very inaccurate. In order to reduce errors due to non-homogenous zero-sequence, the modified takagi allows angle correction if the user knows the system source, the zero-sequence current $(\mathrm{I_0})$ can be adjusted by angle T to improve the fault location for a transmission line. The algorithm

minimizes/eliminates the effects of; fault resistance, impact by load and the line charging current.

The angle correction (T) can be calculated by using the zero sequence fault current ($\mathrm{I_{f0}}$) , if the source impedance zero-sequence impedance ($\mathrm{ZS_0 = 3Z_0}$) and ($\mathrm{ZR_0 = Z_0}$) is known [34] . These values can be estimated using fault recorders [35]

$$\frac{I_f}{3 * I_0} = \frac{ZR_0 + (1-m)Z_0}{ZS_0 + ZR_0 + Z_0} = A\angle T \qquad \textit{Eq 17}$$

$$m = \frac{Im(V_s * 3I_0^* * e^{-iT})}{Im(Z_{L1} * I_s * 3I_0^* * e^{-iT})} \qquad \textit{Eq 18}$$

Fault location Algorithm by Saha

A fault point in a three phase transmission line is determined by measurement of current and voltage data at both side of the transmission line. In this algorithm the fault type; single-phase/multi-phase ground fault/phases-to phase fault is determined and the parameters in a quadric equation are used to calculate distance to fault on a transmission line. The equation is based from the electrical relationship, between the complex values of the line impedance, the source impedance, and current and voltage. The equation eliminates the use of fault resistance and possible zero-sequence components. The parameters are determined by the type of fault and the equation is solved by means of a numerical square root method [30] [39] [B.1.].

Fault location equation by Saha, notify that the values for $(\mathrm{V_s})$, $(\mathrm{I_s})$ and $(\mathrm{I_{fs}})$ are different for each fault type according to (*Table 1*).

$$V_s = I_s * m * Z_L + I_{fs} * (\frac{R_f}{D}) \qquad \textit{Eq 19}$$

$$D = \frac{(1-m) * Z_L + Z_s}{Z_s + Z_L + Z_R} \qquad \textit{Eq 20}$$

The line section $(\mathrm{Z_L})$ is a known parameter and $(\mathrm{Z_s})$ may be known, but not if the parameter can be calculated by the measured values of current and voltages at the bus bar *(S).*

Input value $(\mathrm{Z_R})$ may also be unknown; the parameter should be estimated with an acceptable degree of accuracy [39] the variable (D) is the distributions factor for the positive sequence and negative sequence networks.

$Z_L = The\ impedance\ of\ the\ line\ section$

$Z_s = Source\ impedance\ of\ network\ lying\ behind\ the\ section\ (near\ end)$

$Z_R = Source\ impedance\ of\ network\ lying\ ahead\ of\ the\ section\ (remote\ end)$

$I_{fs} = Current\ change\ at\ point\ S\ due\ to\ the\ fault\ (\ I_{fs} = D * I_f)$

Since equation of parameter (D) is a linear function of m the general equation will be non-linear and written as follows (*Eq 21).*

$$m^2 - m * K_1 + K_2 - K_3 * R_f = 0 \qquad \textit{Eq 21}$$

Where:

$$K_1 = \frac{V_s}{I_s * Z_L} + 1 + \frac{Z_R}{Z_L} \qquad \textit{Eq 22}$$

$$K_2 = \frac{V_s}{I_s * Z_L} * \left(\frac{Z_R}{Z_{L1}}\right) + 1 \qquad \textit{Eq 23}$$

$$K_3 = \frac{I_{fs}}{I_s * Z_L} * \left(\frac{Z_s + Z_R}{Z_L} + 1\right) \qquad \textit{Eq 24}$$

The values of $(\mathrm{V_s})$, $(\mathrm{I_s})$ and $(\mathrm{I_{fs}})$ may be calculated from current and voltages measured locally at the end point S according (*Table 1)* .The distribution factors of $(\mathrm{K_1}), (\mathrm{K_2})$ and $(\mathrm{K_3})$ is a complex factor and by separate the complex equation into real and imaginary parts, the unknown fault resistance The real and imaginary parts of the complex factors $(\mathrm{R_f})$ can be eliminated.

$$m^2 + B * m + C = 0 \qquad \textit{Eq 25}$$

Where:

$$B = \frac{Re(K_1) * Im(K_3) - Im(K_1) * Re(K_3)}{(Re(K_3)} \qquad \textit{Eq 26}$$

$$C = \frac{Im(K_2) * Re(K_3) - Re(K_2) * Im(K_3)}{Re(K_3)} \qquad \textit{Eq 27}$$

When solving equations relative distance to fault:

$$m_1 = \frac{-B + \sqrt{B^2 - 4C}}{2} \qquad \textit{Eq 28}$$

$$m_1 = \frac{-B - \sqrt{B^2 - 4C}}{2} \qquad \textit{Eq 29}$$

The Saha algorithm can also be written as following quadratic equation with use of symmetrical components:

$$A_2 m^2 + A_1 m + A_0 + A_{00} * R_f = 0 \qquad \textit{Eq 30}$$

Transmission network with single lines complex coefficients used for determining fault current distribution factor for positive and negative-sequence.

Where:

$$A_2 = -Z_{L1} * Z_{L1} \qquad \textit{Eq 31}$$

$$A_1 = (Z_{L1} + Z_{R1}) - \left(-Z_{L1} * \frac{V_s}{I_s}\right) \qquad \textit{Eq 32}$$

$$A_0 = Z_{L1} * \frac{V_s}{I_s} \qquad \textit{Eq 33}$$

$$A_{00} = Z_{S1} + Z_{R1} + Z_{L1} * (\frac{I_{sup}}{I_s}) \qquad \textit{Eq 34}$$

Equation *(Eq* 35) will be calculated as following to eliminate use of $(\mathrm{R_f})$*:*

$$B_2 m^2 + B_1 m + B_0 = 0 \qquad \textit{Eq 35}$$

Where:

$$B_2 = Re(A_2) * Im(A_{00}) - Im(A_2) * Re(A_{00}) \qquad \textit{Eq 36}$$

$$B_1 = Re(A_1) * Im(A_{00}) - Im(A_1) * Re(A_{00}) \qquad \textit{Eq 37}$$

$$B_0 = Re(A_0) * Im(A_{00}) - Im(A_0) * Re(A_{00}) \qquad \textit{Eq 38}$$

Relative distance to fault when solving equation (*Eq 39/Eq 40*) with use of symmetrical components:

$$m_1 = \frac{(-B_1 - \sqrt{{B_1}^2 - 4B_2 * B_0})}{2B_2} \quad \textit{Eq 39}$$

$$m_1 = \frac{-B_1 + \sqrt{{B_1}^2 - 4B_2 * B_0}}{2B_2} \quad \textit{Eq 40}$$

Fault location algorithm by Wisziewski

Fault location algorithms by Wisziewski are based on standard calculations of line resistance; reactance and the correction error by the fault resistance. The algorithm utilizing the general fault loop model and the general formula of calculation fault current, and the apparent resistance and reactance measurement at one end of the line. In cases of interphase short-circuits the fault resistance in general very low, therefore the expected errors are also limited. In cases of ground fault high fault resistance may be assumed; hence the errors affect the precision of short circuit location [16] .

The general formula of the algorithm uses calculation of fault loop model of resistance and reactance measured by the fault recorder or distance relay.

$$Z_{sp} - mZ_{l1} - \frac{R_f}{k_1} * \frac{I_{sup}}{I_s * e^{-i\gamma}} \quad \textit{Eq 41}$$

The input signal is available at one end of the line; it can be assumed that the phase angle γ of the line impedance and phase angle of the distributed factor (d) are known. Now we separate the imaginary and real part separately.

$$Z_{sp} = \frac{V_{sp}}{I_{sp}} = R_{sp} + iX_{sp} \quad \textit{Eq 42}$$

$$R_{sp} - mR_{L1} - \frac{R_f}{k_1} a = 0 \quad \textit{Eq 43}$$

$$X_{sp} - mX_{L1} - \frac{R_f}{k_1} b = 0 \quad \textit{Eq 44}$$

Where:

$$a = real\left(\frac{I_{sup}}{I_s * e^{-iT}}\right) \quad \textit{Eq 45}$$

$$b = Imag\left(\frac{I_{sup}}{I_s * e^{-iT}}\right) \quad \textit{Eq 46}$$

To eliminate the unknown term (R_f/k_1) from above equation, the condition of symmetrical components $(X_{L1}/R_{L1} = \tan(\phi))$ may be utilized [8].

The following equation forms a solution of the set of equations is as follows [8].

$$d = \frac{X_{sp}}{X_{L1}} - \frac{\frac{R_{sp}}{X_{L1}} * tan(\phi) - \frac{X_{sp}}{X_{L1}}}{\frac{a}{b} * tan(\phi) - 1} \qquad Eq\ 47$$

Two-Ended fault location algorithm

Two-ended fault location estimation is fundamentally similar to the one-terminal algorithm. But the method can improve the accuracy of fault distance measurements significantly by using data from the two ends of the line to cancel the effect of fault resistance and infeed [3]. Two-end and multi-end fault location algorithms divided in two main categories, unsynchronized and synchronized measurement. The algorithms process signals from both terminals of the line and a large amount of information is utilized. Therefore, performance of the two-end algorithm is generally superior in comparison to the one-end approaches [24]

Two end Negative sequence method

The developed algorithm in [30] uses negative-sequence voltage obtained from both side of its symmetrical components at the fault point. By using negative-sequence components, the effects of pre-fault power flow and fault resistance are eliminated. Unlike one-end methods, negative sequence requires source impedance to perform fault location estimation.

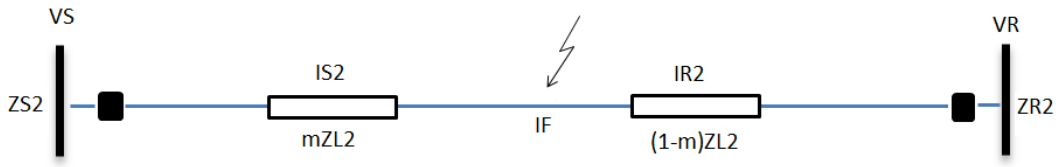

Figure 12: *Single transmission model and illustration of input data.*

The general formula of the algorithm uses calculation from both sides of the transmission line with elimination of the fault voltage(V_f).

At S-side:

$$V_f = -I_{S2} * (Z_{S2} + mZ_{L2}) \qquad Eq\ 48$$

At R-side:

$$V_f = -I_{R2} * (Z_{R2} + (1 - m)Z_{L2}) \quad \textit{Eq 49}$$

By eliminating fault voltage, the resulting expression follows:

$$|I_{R2}| = \frac{|(I_{S2} * Z_{S2}) + m * (I_{S2} * Z_{L2})|}{|(Z_{R2} * Z_{L2}) - m * Z_{L2})|} \quad \textit{Eq 50}$$

The further equation simplifies above formula, and the expanding rearranging term produces a quadratic equation of the form with following input but first separate the imaginary part from the real part [42] [30]

Where:

$I_{S2} * Z_{S2} = a_1 + jb_1$

$I_{S2} * Z_{L2} = a_2 + jb_2$

$Z_{R2} * Z_{L2} = a_3 + jb_3$

$Z_{L2} = a_4 + jb_4$

$$A * m^2 + B * m + C = 0 \quad \textit{Eq 51}$$

Equation (Eq 51) is solved for distance to fault (m) using quadratic solution model. The coefficients (A), (B) and (C) are given below.

Where:

$A = |I_{R2}|^2 * (a_4 + jb_4)^2 - (a_2 + jb_2)^2$

$B = -2 * |I_{R2}|^2 * (a_3 * a_4 + jb_3 * jb_4) - 2(a_1 * a_2 + jb_1 * jb_2)$

$C = |I_{R2}|^2 * (a_3 + jb_3)^2 - (a_1 + jb_1)^2$

Two end Three Phases Impedance Matrix Method

Fault location model based on three phase line impedance matrix, the method is applicable to transmission lines and distributed feeders [42]. The method is independent of fault type and insensitive to source impedance variation or fault resistance. Using the one-line diagram (*Figure 12*), the voltage and terminal lines can be expressed as two formulas one on each side of the lines. In the formula of the algorithm both synchronized data can be used as unsynchronized to calculate distance to fault. Assuming that the phasors of the three-phase current and voltage at S-side and R-side are synchronously obtained, the three-phase vector of current and voltage at each side can be expressed as:

At S-side:

$$V_{Sabc} = m * Z_{Labc} * I_{Sabc} * V_{fabc} \quad \textit{Eq 52}$$

At R-side

$$V_{Rabc} = (1 - m) * Z_{Labc} * I_{Rabc} * V_{fabc} \quad \textit{Eq 53}$$

Where:

$$V_{Sabc} = \begin{pmatrix} V_{Sa} \\ V_{Sb} \\ V_{Sc} \end{pmatrix}$$

$$I_{sabc} = \begin{pmatrix} I_{Sa} \\ I_{Sb} \\ I_{Sc} \end{pmatrix}$$

$$V_{Rabc} = \begin{pmatrix} V_{Ra} \\ V_{Rb} \\ V_{Rc} \end{pmatrix}$$

$$I_{Rabc} = \begin{pmatrix} I_{Ra} \\ I_{Rb} \\ I_{Rc} \end{pmatrix}$$

$$Z_{Labc} = \begin{pmatrix} Z_{aa} & Z_{ab} & Z_{ac} \\ Z_{ab} & Z_{bb} & Z_{bc} \\ Z_{ca} & Z_{cb} & Z_{cc} \end{pmatrix}$$

$$V_{fabc} = \begin{pmatrix} V_{fa} \\ V_{fb} \\ V_{fc} \end{pmatrix}$$

The algorithm assumes that the phasors of the three phases current and voltages at S-Side and R-side are synchronously obtained [8] Subtracting equation (Eq 52) from (Eq 23) we obtain.

$$V_{Sabc} - V_{Rabc} + Z_{Labc} * I_{Rabc} = m * Z_{Labc} (I_{Sabc} + I_{Rabc}) \quad \textit{Eq 54}$$

Equation (Eq 54) can be written as:

$$Y = V_{Sabc} - V_{Rabc} + Z_{Labc} * I_{Rabc} \quad \textit{Eq 55}$$

$$M = Z_{Labc} (I_{Sabc} + I_{Rabc}) \quad \textit{Eq 56}$$

The above equation contains three complex equations and six real equations, least-square estimation can be applied to determine the only unknown parameter.

$$m = (\mathrm{conj}(\mathrm{M}) * \mathrm{M})^{-1} * (\mathrm{conj}(\mathrm{M}) * \mathrm{Y}) \qquad Eq\ 57$$

Impedance matrix method is not affected by fault resistance. The technique is general for any type of fault. No fault classification is required. Using the impedance matrix method for fault location is certainly advantageous when data is available at line terminal [8]

Chapter five

Research Methodology of Simulink Model

Simulations and verification of the algorithms accuracy and methodology are an important task in order to create a reliable tool for future simulations and calculation. All algorithms have various weaknesses in the distance to fault calculations. In order to document and verify the weaknesses and strengths of each algorithm a simulation model has been developed in Simulink. The Implementation of five one-side algorithms and three two-side algorithms in the model will create an understanding of selected algorithms in fault location analysis.

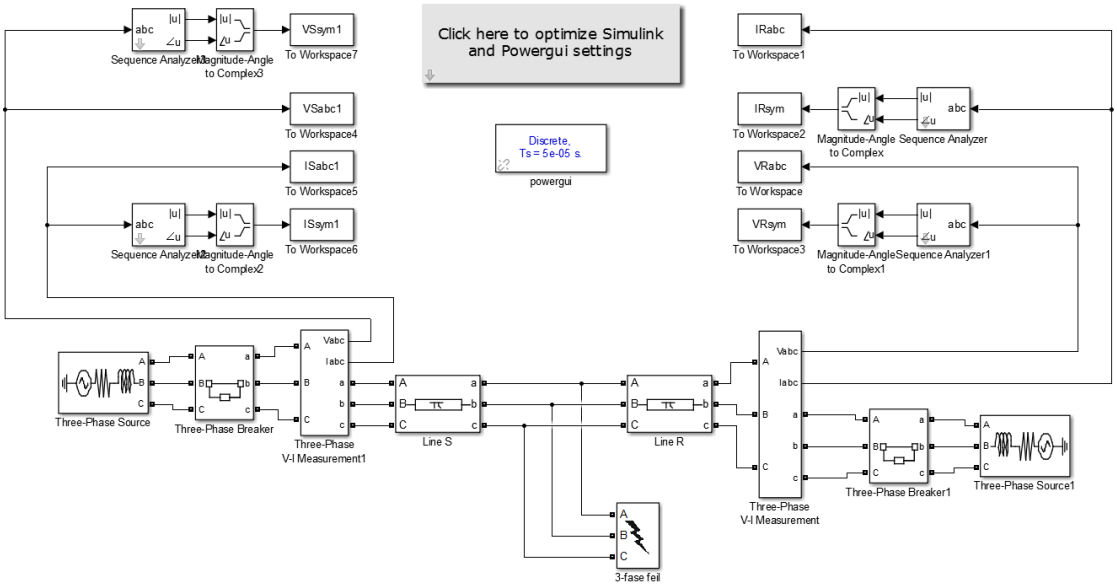

Figure 13: Simulink model for verification of distance to fault algorithms.

Simulations design

The model has two substations with a three-phase source at each side, and the power flows from S-side to the R-side according to *(Figure 13*). Simulation model is developed with variable input value and the data is imported to the MATLAB model for calculation of distance to fault.

The nominal voltage on S-side is set to 420 kV with a three phase short circuit value at 2000 MVA. The nominal voltage on R-side is set to 420 kV with a three phase short circuit value at 1800 MVA, to create a power flow from S-side to R-side of the model the phase angel is set to -10 degree on R-side.

Nominal value in the model is typical value for a transmission grid at designated voltage levels. Print-screen of nominal value is presented visual in *(Figure 14, Figure 15)* below.

S-Side

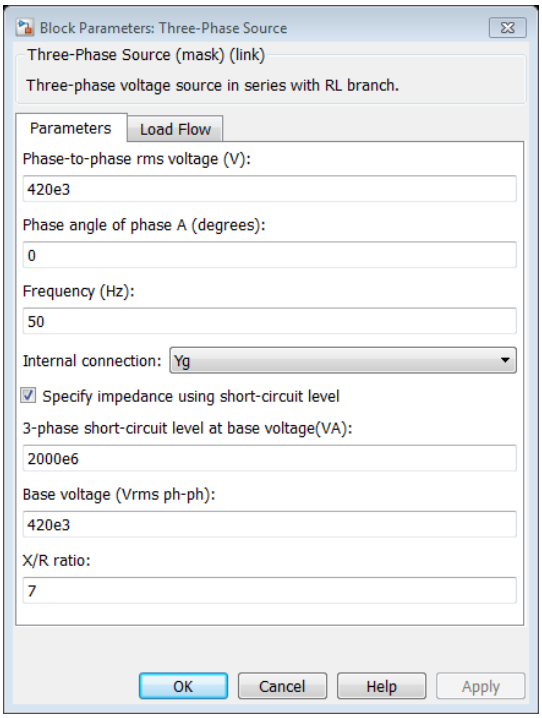

Figure 14: Input value S-side

R-Side

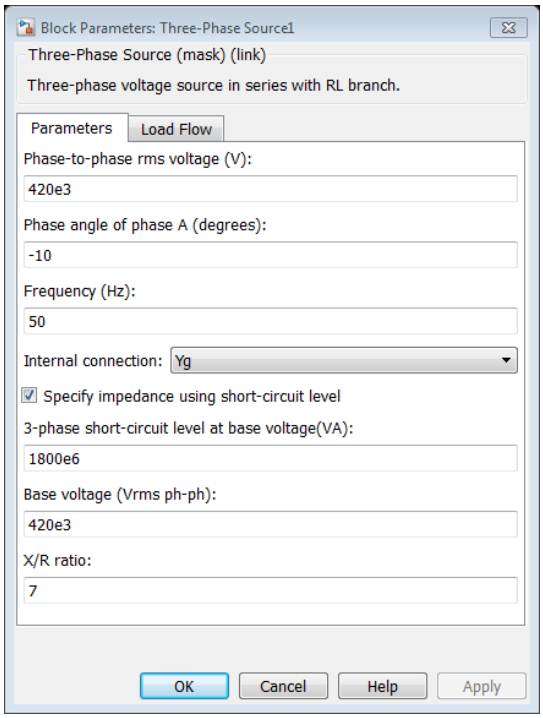

Figure 15: Input value R-side

The transmission line of the Simulink model use a pi-line model with inputs for positive, negative and zero-sequence components of $(R), (C), (L)$ the line length is variable and compared with different verification case.

Line Parameter S-Side

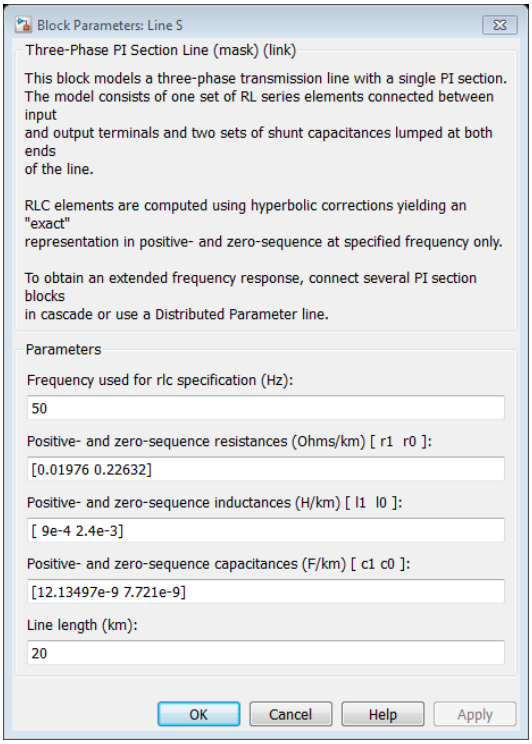

Figure 16: Input value transmission line model S-side

Line Parameter R-side

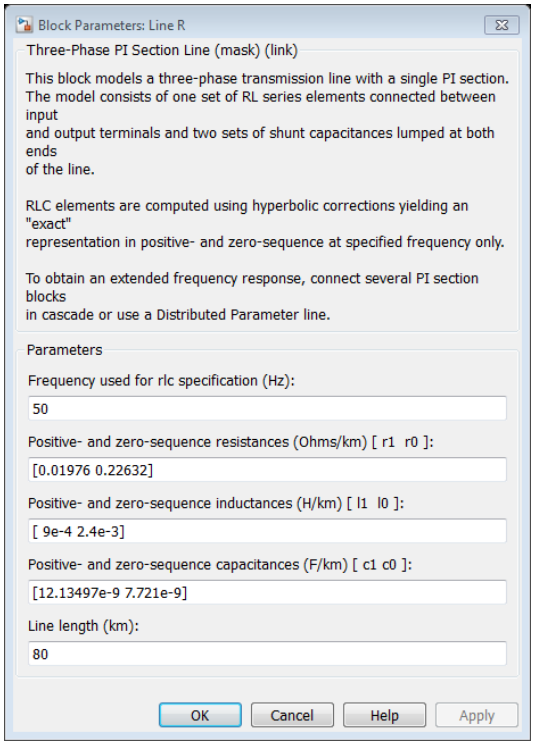

Figure 17: Input value transmission line model R-side

Three phase fault parameter is also variable and the switching time is synchronized with the breakers for each side of the model.

Three-Phases Fault Parameter

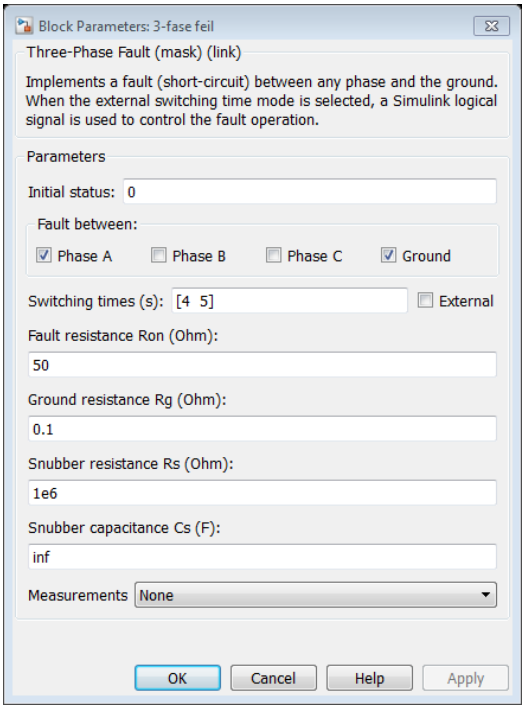

Figure 18: Input value for three-phase fault.

Verification of Algorithm in Simulink

The results of the fault location estimated are listed in two cases, one for one-ended calculation and one other for two-ended calculations. The following results are listed in different table below and present as A-G fault (line-to-Ground fault), B-C fault (line-to-line fault), A-B-G (line-to-line-to ground fault) and A-B-C fault (line-to-line-to-line fault).

Fault location verification

Different types of fault are applied to the transmission line. The location of the fault is selected to 51 % of the total length and the fault resistance is chosen to $(0{,}1\ \Omega)$, $(5\ \Omega)$, $(10\ \Omega)$, $(30\ \Omega)$, $(50\ \Omega)$ to demonstrate the effect to the fault location estimation. The duration of fault is 0.9 seconds, previous example show the implementation of this in Simulink simulation. Fault location estimations for different fault with various fault resistance are presented.

Transmission line length	97,8 km
Distance to fault	51,1 %

Ground fault

Fault location estimation for A-G fault with different fault resistance, with a fault 51 % of the total transmission line length (100km) is presented below.

Ground fault current depends on the networks sequence admittance and the fault resistance, were fault resistance depends on the earth condition and the fault parameters. The fault resistance might have significant effect on the earth fault characteristics. When a fault occurs to the overhead lines steel tower or grounded pole the footing system resistance is included automatically in the fault circuit and the resulting ground current may be less than the calculated neglecting fault resistance. The ground fault current is equal to the sum of positive, negative and zero-sequence systems reactance to the point of fault. Because of the tower footing the fault resistance may be as high as 10 Ω. In case of broken conductor or fallen trees result in a higher fault resistance [7]

Presented algorithm accuracy depends on the compensation of the zero sequence components and the majority of faults that occurs on the transmission system ground faults.

A-G fault	Takagi	Modified takagi	Wisziewski	Novosel	Harrysson
$R_f = 0{,}1\ \Omega$	50,80 %	49,43 %	51,00 %	50,31 %	50,95 %
$R_f = 5\ \Omega$	50,86 %	47,05 %	52,21 %	51,17 %	50,92 %
$R_f = 10\ \Omega$	50,66 %	44,85 %	53,41 %	53,00 %	50,84 %
$R_f = 30\ \Omega$	50,56 %	NA %	56,90 %	57,05	50,77 %
$R_f = 50\ \Omega$	49,90 %	NA %	58,64 %	59,38 %	49,99 %

Table 2: *A-G Fault location estimation result from Simulink one-end fault location*

At an increasing fault resistance, the effect of the algorithm Takagi and Harrysson creates large swings in the calculation method, the peak value of these oscillations agree very well with the expected results (51 %). Therefore, peak value of these oscillations as unequivocal answer in the verification presentation.

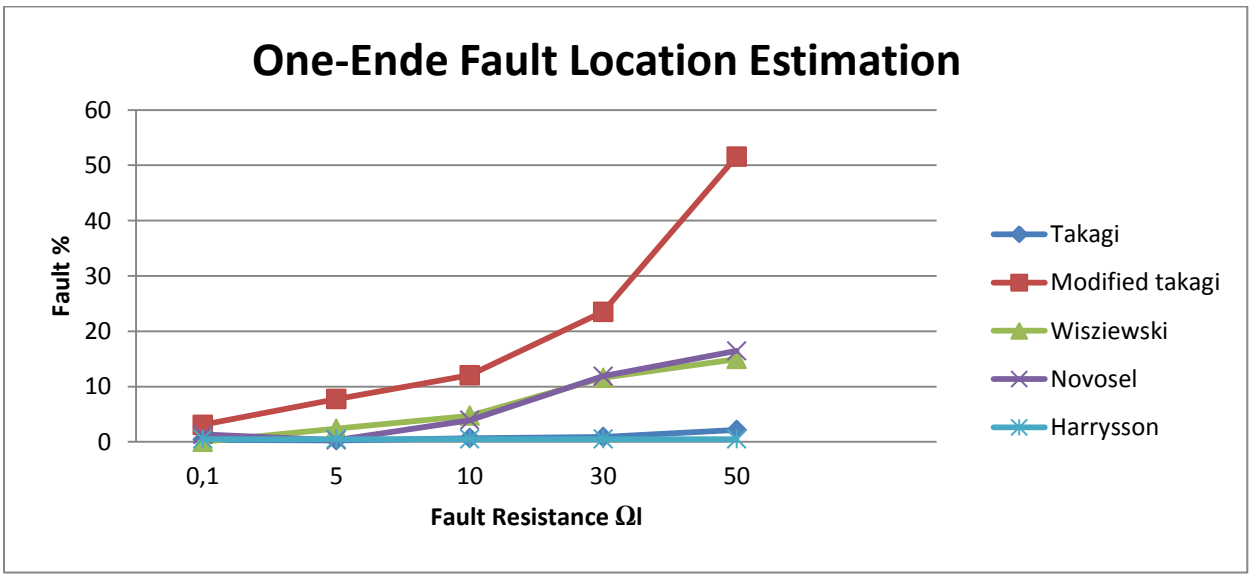

Figure 19: fault statistics with an increasing fault resistance.

A-G fault	Negative-Sequence	Saha One	Modified Saha	Impedance matrix
$R_f = 0{,}1\ \Omega$	49,35 %	59,02 %	56,3 %	51,32 %
$R_f = 5\ \Omega$	49,9 %	60,00 %	54,9 %	50,05 %
$R_f = 10\ \Omega$	48,22 %	57,65 %	60,60 %	48,52 %
$R_f = 30\ \Omega$	49,06 %	NA	NA	42,39 %
$R_f = 50\ \Omega$	45,55 %	NA	NA	38,25 %

Table 3: A-G Fault location estimation result from Simulink two-end fault location

Above table shows fault location estimation for A-G fault with different fault resistance. Two-ended fault location methods Impedance matrix and negative-sequence are very accurate at any fault resistance up to $(10\ \Omega)$. Algorithm Saha One and Modified Saha accuracy is lower with accuracy within 5-18 % of fault estimation at a low fault resistance.

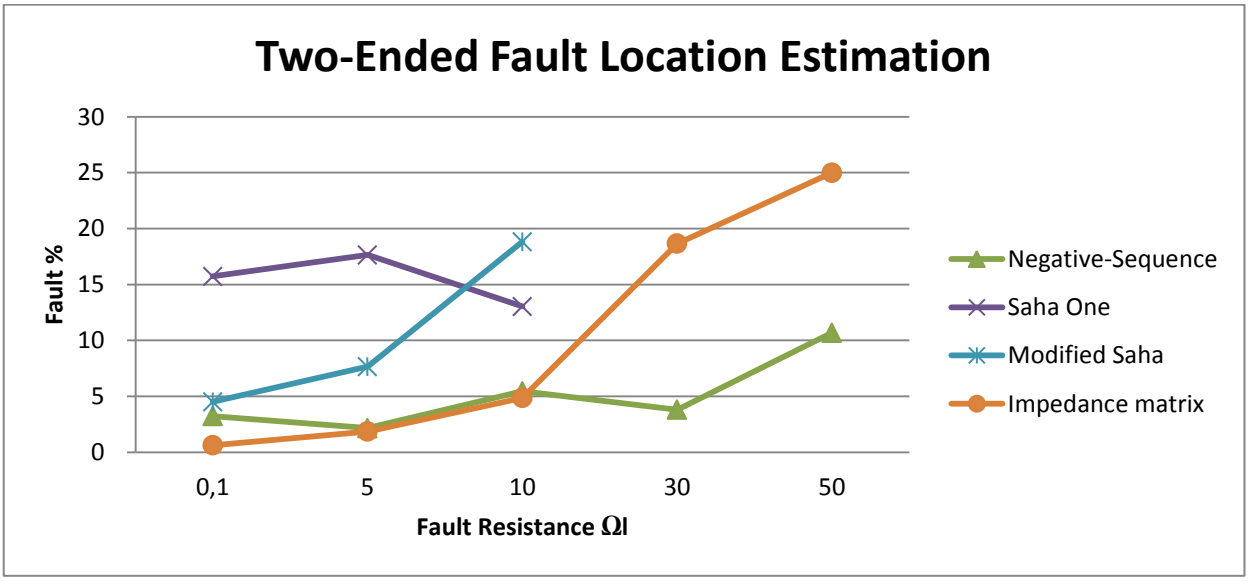

Figure 20: fault statistics with an increasing fault resistance.

A-B-G fault	Takagi	Modified takagi	Wisziewski	Novosel	Harrysson
$R_f = 0{,}1\ \Omega$	50,99 %	49,96 %	50,03 %	50,00	50,90 %
$R_f = 5\ \Omega$	50,76 %	49,94 %	46,93 %	47,03 %	50,70 %
$R_f = 10\ \Omega$	50,46 %	48,77 %	43,88 %	43,88 %	50,46 %
$R_f = 30\ \Omega$	50,88 %	NA	NA	NA	50,80 %
$R_f = 50\ \Omega$	51,39 %	NA	NA	NA	51,20 %

Table 4: A-B-G One-ended fault location estimation result from Simulink

For interphases fault with ground fault all presented algorithms show a margin fault result with a small deviation from distance to fault location. At a higher fault resistance $(30\ \Omega)$ Modified takagi, Wisziewski and Novosel indicated an incorrect result with negative percentage deviation.

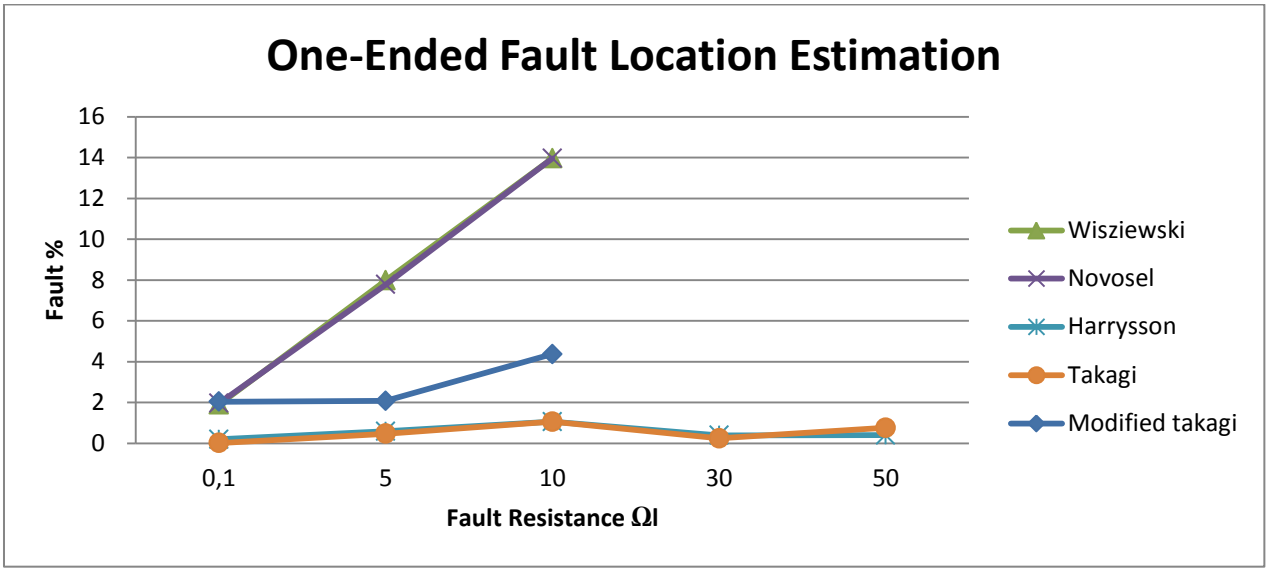

Figure 21: fault statistics with an increasing fault resistance at A-B-G fault.

A-B-G fault	Negative-Sequence	Saha One	Modified Saha	Impedance matrix
$R_f = 0{,}1\ \Omega$	46,33 %	56,22 %	68,25 %	49,98 %
$R_f = 5\ \Omega$	45,88 %	79,88 %	62,83 %	51,63 %
$R_f = 10\ \Omega$	45,15 %	NA	69,8 %	51,75 %
$R_f = 30\ \Omega$	41,65 %	NA	51,85	51,80 %
$R_f = 50\ \Omega$	38,45 %	NA	NA	51,86 %

Table 5: A-B-G Two-ended fault location estimation result from Simulink

Two ended algorithms Impedance matrix have high accuracy and are almost independent of fault resistance. Saha One and Modified Saha have high fault margin from known distance to fault location.

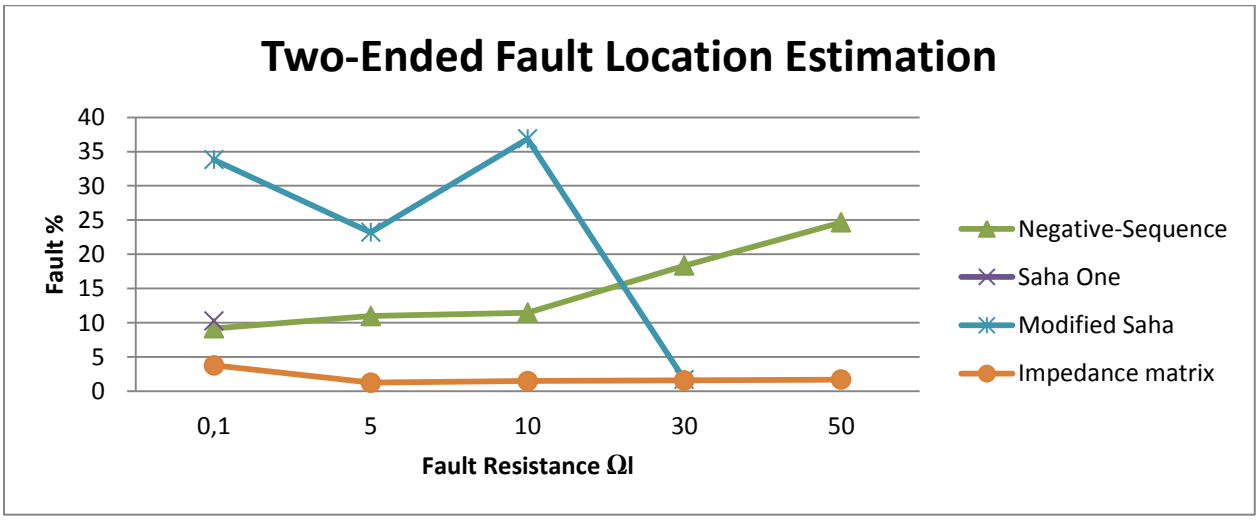

Figure 22: fault statistics with an increasing fault resistance at A-B-G fault.

Interphase faults

Fault location estimation for B-C and A-B-C fault with different fault resistance, with a fault 51 % of the total transmission line length (100km) is presented below.

In cases of interphase short-circuit fault are the fault resistance generally low and do not exceed 0.5 Ω [7] . In phases-to-phase faults resistance is due to the arc-resistance, the arc-resistance is dependent on the magnitude of the fault current, thus in reality it will not be constant for the different fault location. Large short circuits current means a smaller arc-resistance, so the arc-resistance will be smaller for a phase-to-phase fault close to the substation.

B-C fault	Takagi	Modified takagi	Wisziewski	Novosel	Harrysson
$R_f = 0{,}1\ \Omega$	51,00 %	NA	50,03 %	49,99 %	51,00 %
$R_f = 5\ \Omega$	50,76 %	NA	47,03 %	47,04 %	50,88 %
$R_f = 10\ \Omega$	50,40 %	NA	43,88 %	43,87 %	50,46 %
$R_f = 30\ \Omega$	49,88 %	NA	29,97 %	29,98 %	49,88 %
$R_f = 50\ \Omega$	49,39 %	NA	NA	NA	49,39 %

Table 6: B-C One–ended fault location estimation result from Simulink simulation.

Above table shows fault location estimation for B-C fault with different fault resistance. All implemented one ended algorithms except Modified takagi have high accuracy. Due to previously analysis, Modified takagi algorithm is more suitable for single-phase-to-ground faults. Takagi and Harrysson algorithms use of pre-fault and fault data reduce the effect of load flow and minimizing the effect of fault resistance, therefore higher accuracy.

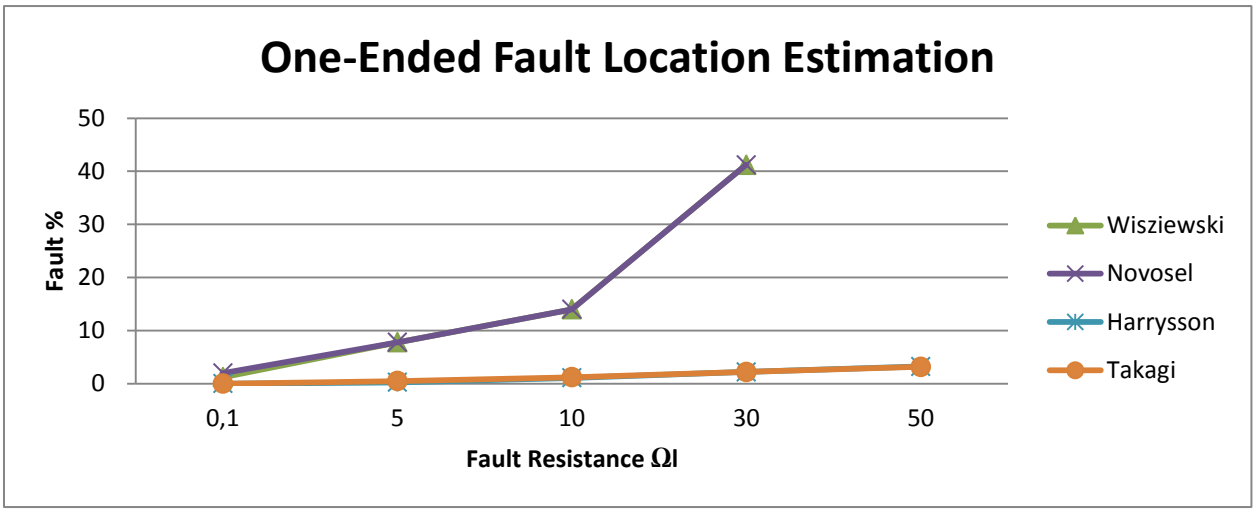

Figure 23: B-C fault calculation of different methods fault margin at specific known fault resistance.

B-C fault	Negative-Sequence	Saha One	Modified Saha	Impedance matrix
$R_f = 0{,}1\ \Omega$	53,18 %	61,14 %	52,84 %	50,01 %
$R_f = 5\ \Omega$	52,70 %	66,65 %	78,85 %	51,21 % %
$R_f = 10\ \Omega$	52,12 %	NA	NA	51,75 %
$R_f = 30\ \Omega$	48,89 %	NA	NA	52,52 %
$R_f = 50\ \Omega$	45,09 %	NA	NA	52,86 %

Table 7 Two-ended fault location estimation result from Simulink simulation

For B-C fault, algorithms Saha One and Modified Saha have high fault high percentage error margin from the estimated distance to the fault. Negative sequence and impedance matrix algorithms have more accuracy at a higher fault resistance.

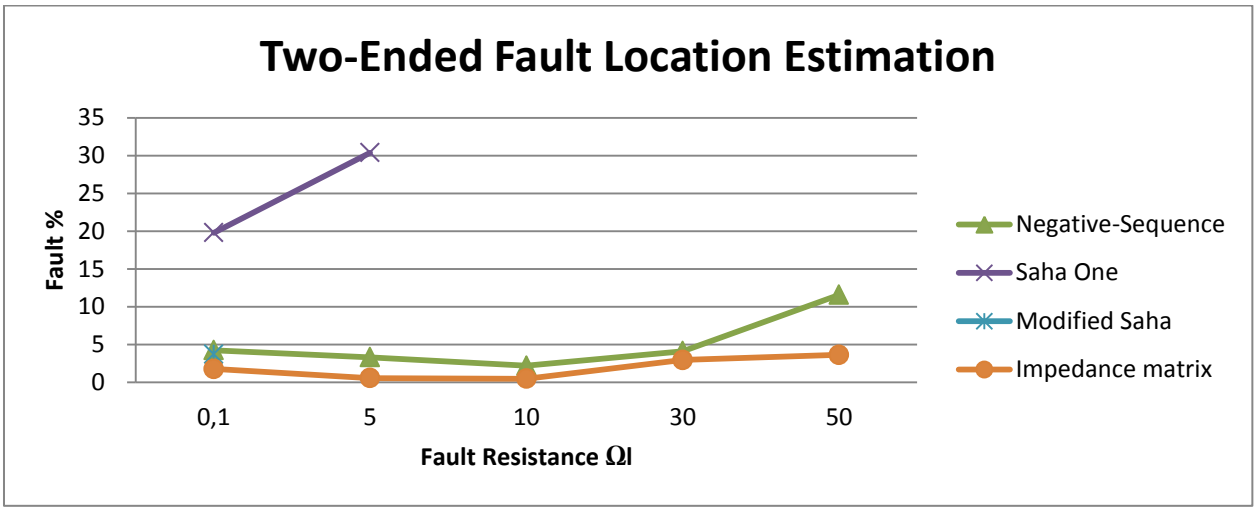

Figure 24: B-C fault calculation of different methods fault margin at specific known fault resistance

A-B-C fault	Takagi	Modified takagi	Wisziewski	Novosel	Harrysson
$R_f = 0{,}1\ \Omega$	50,05 %	NA	50 %	50,02 %	50,04 %
$R_f = 5\ \Omega$	50,55 %	NA	47,42 %	47,05 %	50,66 %
$R_f = 10\ \Omega$	50,14 %	NA	44,00 %	44,38 %	50,18 %
$R_f = 30\ \Omega$	50,80 %	NA	30,5 %	39,98 %	50,78 %
$R_f = 50\ \Omega$	54,89 %	NA	NA	NA	55,00 %

Table 8: A-B-C fault location estimation result from Simulink simulation

As shown in these above tables, the simulated result of a three phase's sources with algorithms; Modified Takagi, Wisziewski and Novosel will have an increased fault location margin with a higher fault resistance, while Takagi and Harrysson methods are almost immune to fault resistance and maintain accurate results in each fault cases.

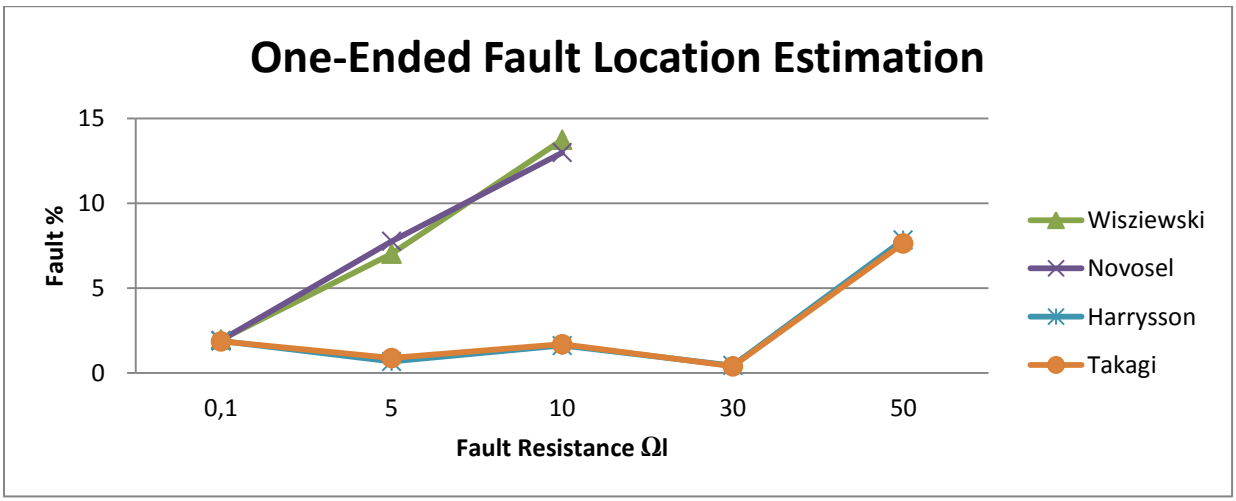

Figure 25: A-B-C fault calculation of different methods fault margin at specific known fault resistance.

A-B-C fault	Negative-Sequence	Saha One	Modified Saha	Impedance matrix
$R_f = 0{,}1\ \Omega$	NA	NA	NA	49,99 %
$R_f = 5\ \Omega$	NA	NA	NA	50 ,00 %
$R_f = 10\ \Omega$	NA	NA	NA	50,01 %
$R_f = 30\ \Omega$	NA	NA	NA	50,05%
$R_f = 50\ \Omega$	NA	NA	NA	50,06 %

Table 9: A-B-C Two-ended fault location estimation result from Simulink simulation

In three phase interphase faults impedance matrix presents high accuracy, and rest of implemented two ended algorithm show a negative result.

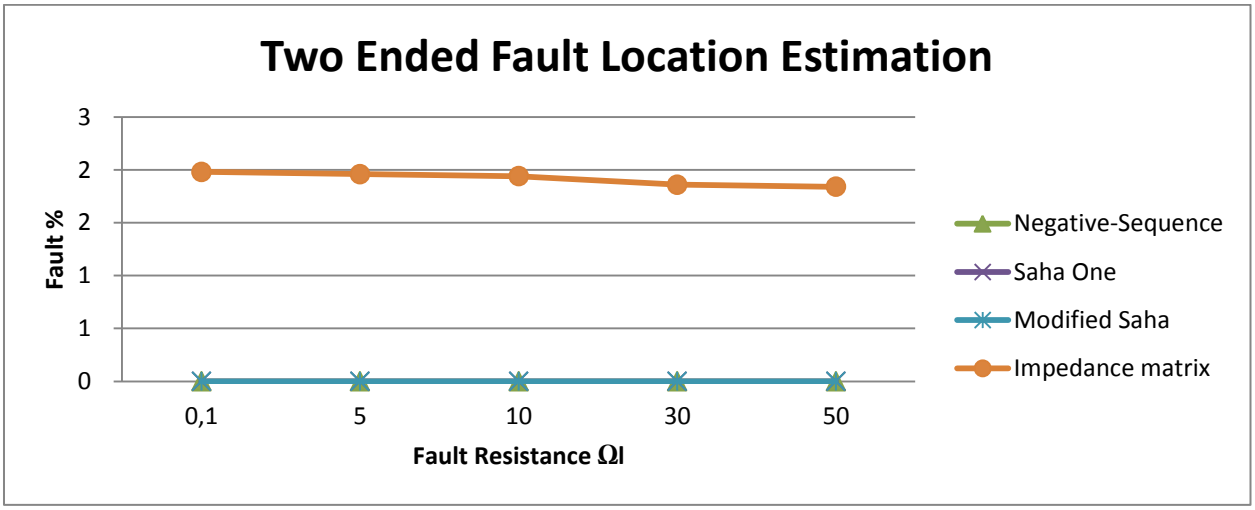

Figure 26: A-B-C fault calculation of different methods fault margin at specific known fault resistance.

Effect of fault resistance

Fault resistance effects the accuracy of short-circuit location, when distance to fault is determined at one or two ends of the transmission line. The effect of the fault resistance occurs because of the current through the fault resistance is phases-shifted compared to the measured current at the end of the line, due to the pre-fault current [16] .

As a result, the fault resistance behaves as apparent impedance with both resistive and reactive components, which is responsible for the error in the fault location with an increased fault resistance. Some methods eliminate the influence of fault resistance and present a good distance to fault accuracy even with an increasing fault resistance. The single line to ground fault shows a better accuracy than the multi-phase fault for most of the testing scenarios.

This verification shows that the apparent resistance measured at one end of the line requires methods with certain corrections to eliminate the fault resistance effect in proportional to the distance to fault.

Field studies – Distance to Fault Calculations

In this chapter, two types of fault cases are simulated and compared for known distance to fault estimation. Calculated results in developed MATLAB model[2] for each fault are then presented and evaluated at each test case.

In the simulation model voltages and current signal are captured by phasor measurer units and fault recorder data at both terminal a transmission lines. Magnitude and angle values are separately illustrated for each phases and specific nominal values from different transmission line are used. Collected data is exported from Gold-digger (Developed by Autodig team) and then imported to MATLAB for fault location estimation.

Fault Case One

Case one presents a phase-to-phase to ground fault on a 420 kV transmission line R1-S1, with presumed fault caused by bad weather and lightning strike. Involved phases are A and B, current and voltages changes during fault are presented in (*Figure 27:*). Transmission line R1-S1 was disconnected at both ends of the distance protection with no consequences for end users. Calculated distance to fault from relays was 41.34 kilometers from S1 and 42.79 km from R1, total length of line is 84, 13 km.

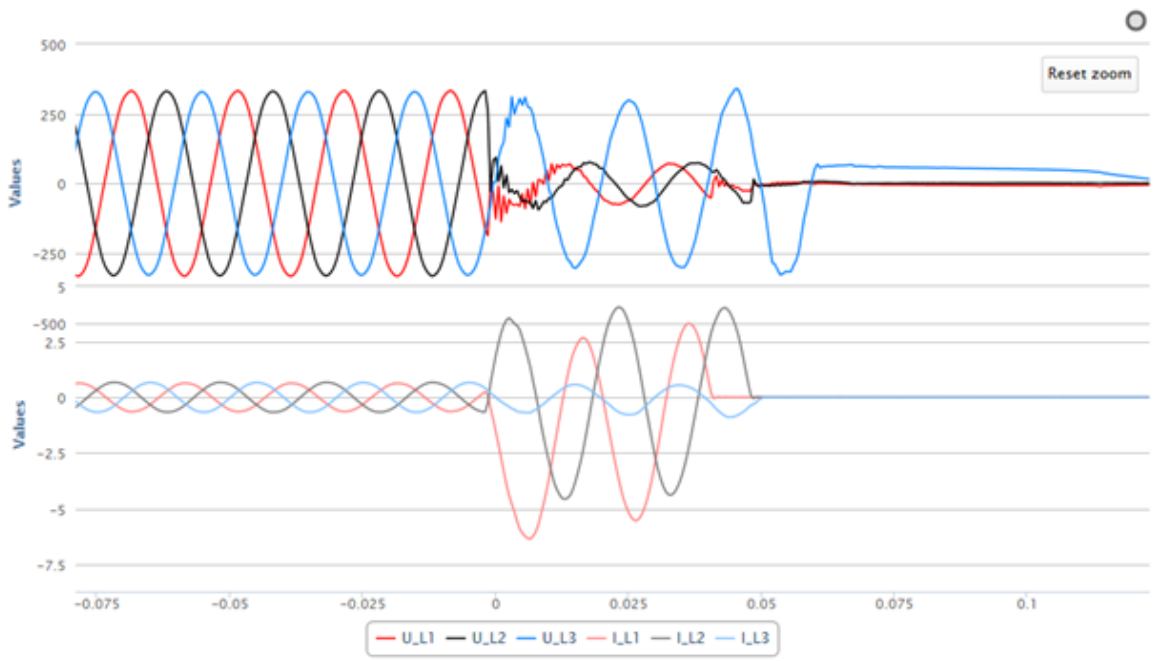

Figure 27: Current and voltages changes during fault.

[2] Appendix A

Simulation result

Case one is simulated with only one-side algorithm. This is because of available data from only one side of the terminal. Calculation of distance to the fault is simulated with the developed model and the results are presented in screenshots below *(Figure 28, Figure 29).*

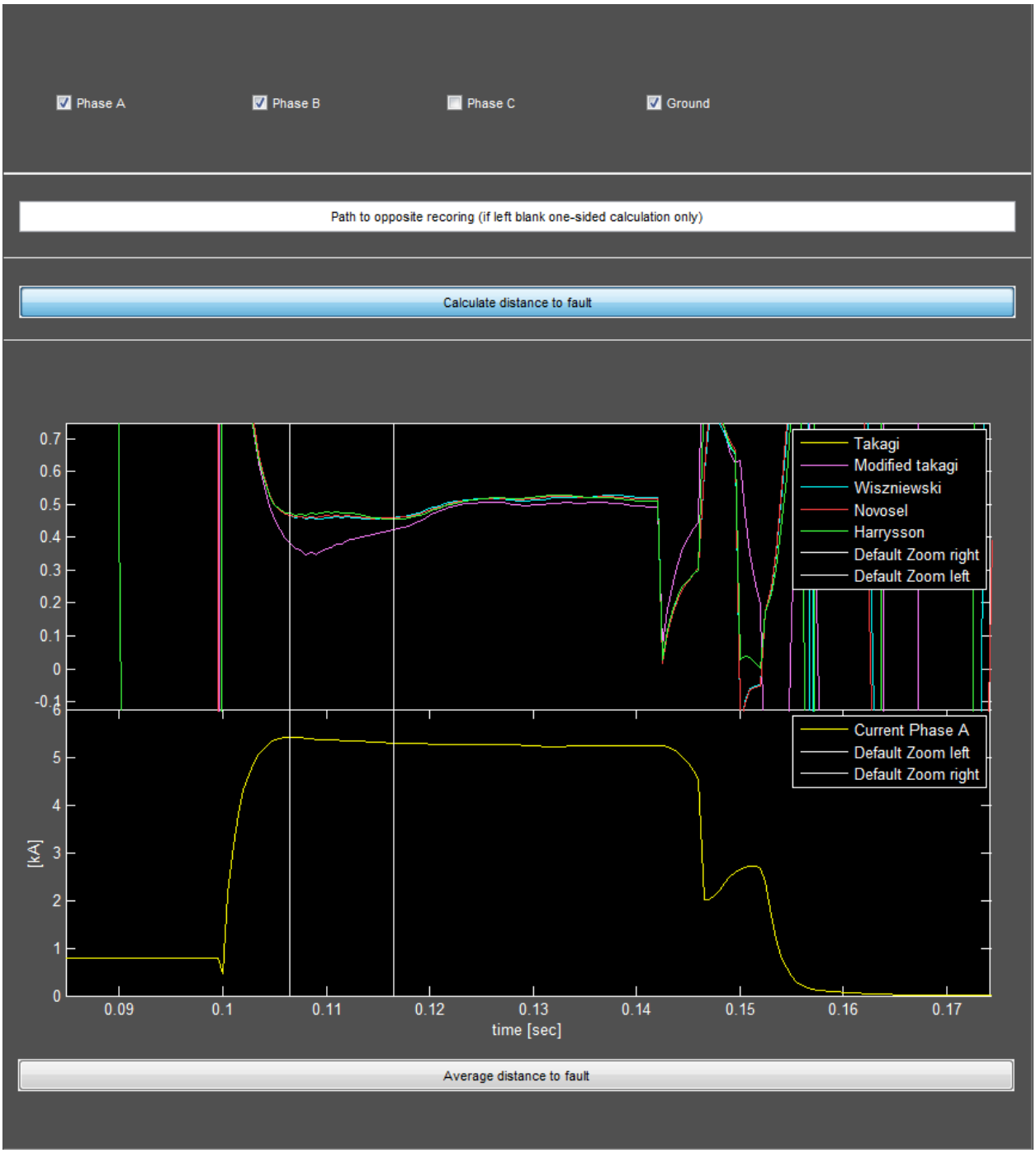

Figure 28: A-B-G fault calculation for one-side implemented algorithms

Above figure shows two graphs; one calculated distance to fault per unit and the other shown the faulted time sequence RMS value of total fault current, this present in phase A minus phase B. Following results of distance to fault calculation are then presented in kilometers for each algorithm in (*Figure 29)* for case one.

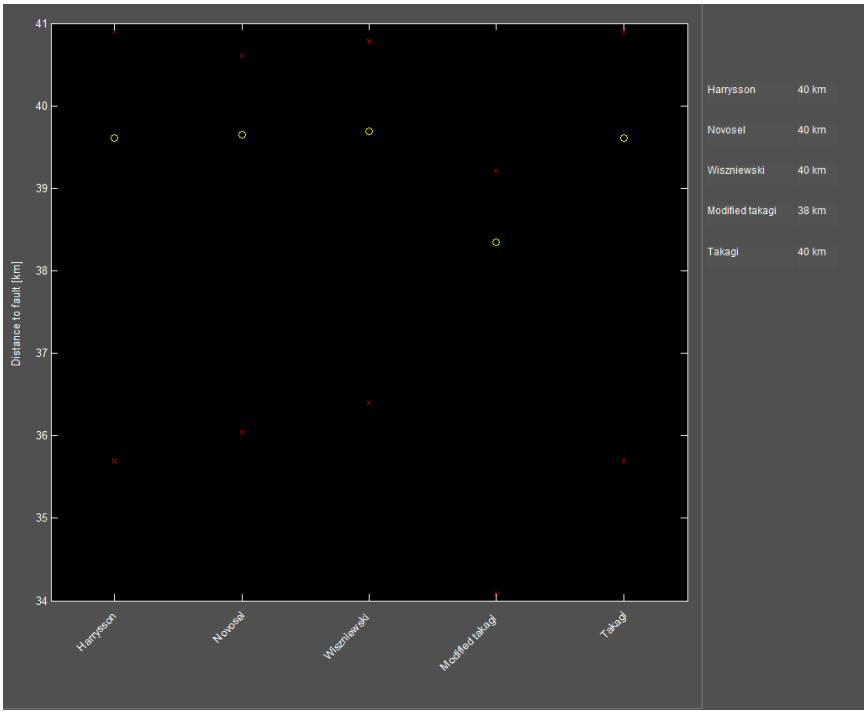

Figure 29: Present graph of calculated distance to fault for each algorithm in kilometers.

Distance to fault calculation with implemented algorithm is made from terminal R1 and the algorithms show god accuracy, compared to known distance to fault 42 34 km.

A-B-G fault	Takagi	Modified takagi	Wisziewski	Novosel	Harrysson
Kilometer	40	38	40	40	40

Table 10: One-side calculations

Fault Case Two

Case two presents phase-to ground fault on a 420 kV transmission lines between RO-H1, fault causes unwanted tripping of power differencing due to incorrect polarity from zero-point current transformer. Protection relays indicate distance to fault 35 km from H1 and 63 km from R0. The error resulted in a 1,200 MW reduction of trading capacity of section H1, and a special regulatory cost of 10 million NOK.

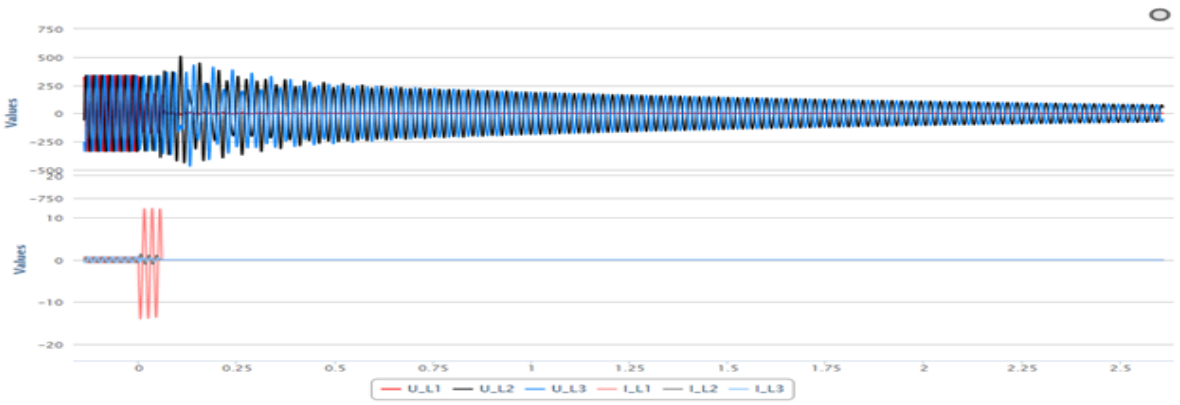

Figure 30: Current and voltages changes during fault.

Simulation result

Case two is simulated with both one-side and two-side calculations. This is because of available data from both sides of the terminal. Calculation of distance to the fault is simulated with the developed model and the results are presented in the screenshots below (*Figure 31, Figure 32).*

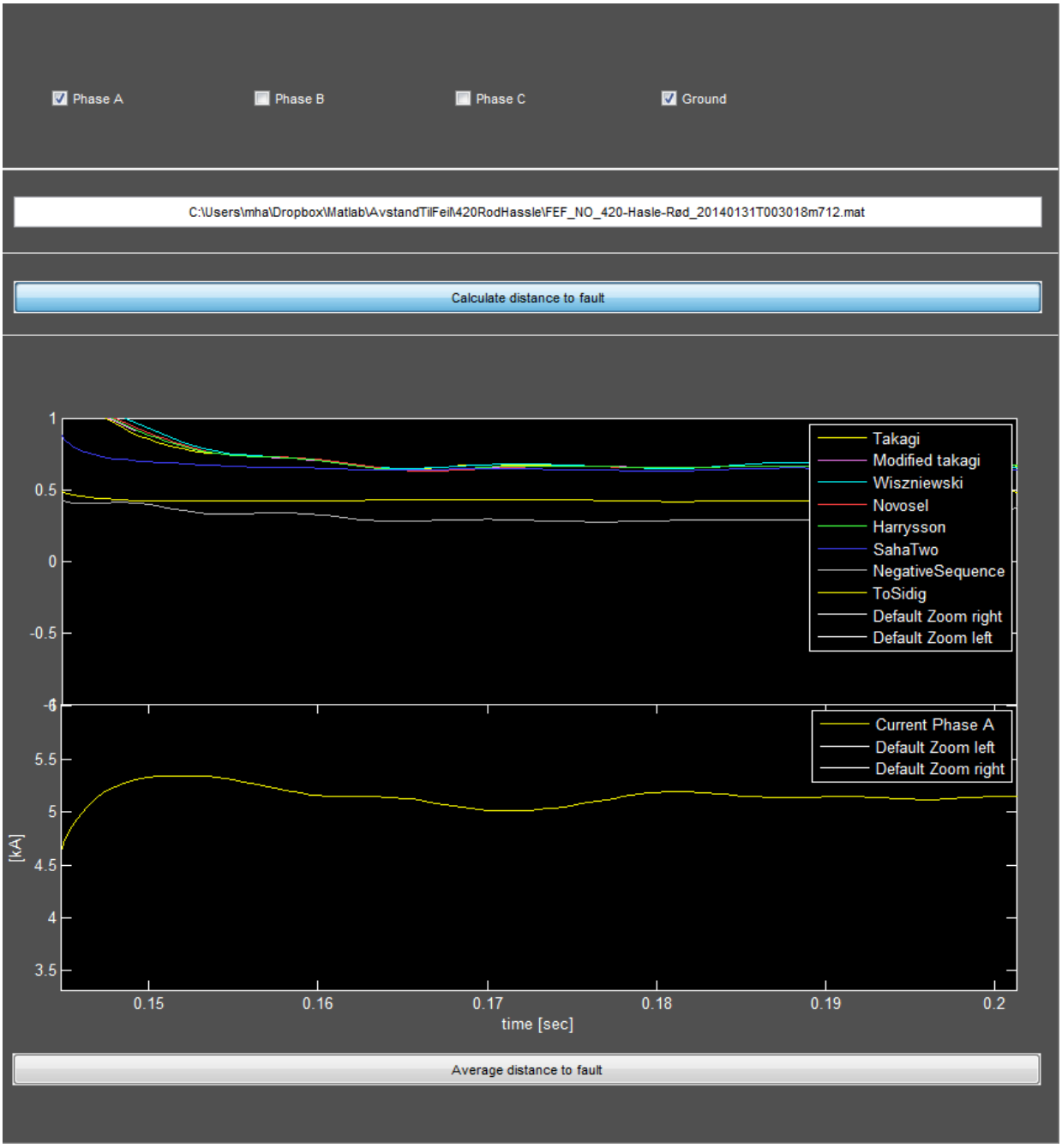

Figure 31 : A-G fault calculation for one-side and two-side algorithms.

Above figure shows two graphs; one calculated distance to fault in per unit and the other shows the faulted time sequence RMS value of total fault current. This is presented in phase A to ground. Following results of calculation are then presented in kilometers for each algorithm in (*Figure 31)* for case two**.**

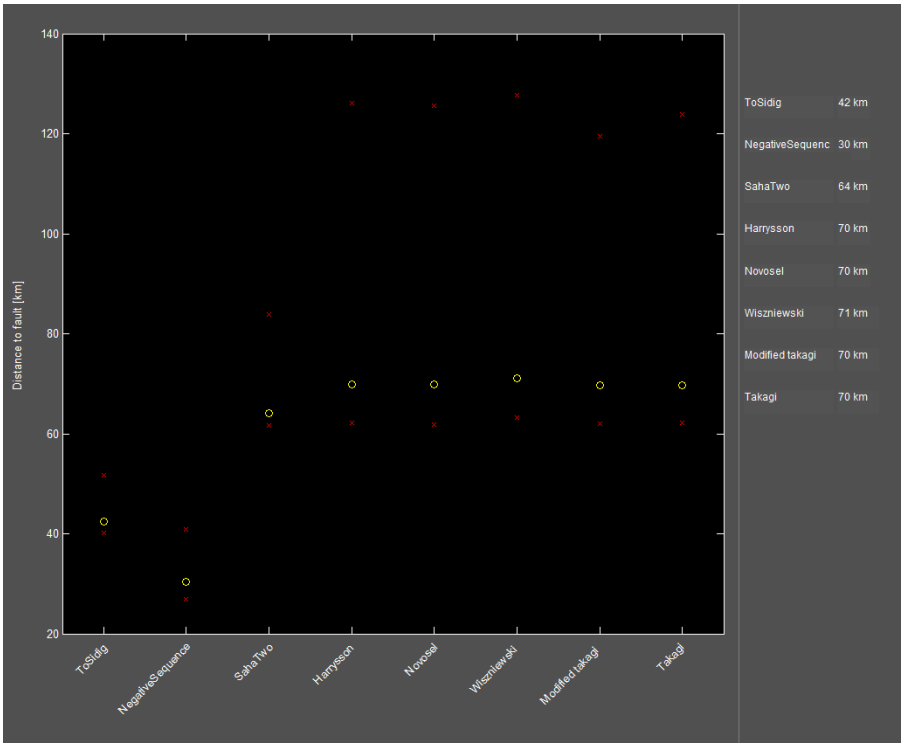

Figure 32: Present graph of calculated distance to fault for each algorithm in kilometers.

Distance to fault calculation with implemented algorithm is made from both terminals. One-side algorithms present a good accuracy, compared to known distance to fault 63 km from R0. Two-side Modified Saha algorithm presents best accuracy of all algorithms with a calculated result of 64 km from R0. Other two-ended algorithms; Impedance matrix and Negative sequence calculated result are presented from terminal H1 to 42 km respective 30 km, compared to known distance to fault 35 km from H1.

A-G fault	Takagi	Modified takagi	Wisziewski	Novosel	Harrysson
Kilometer	70	70	71	70	70

Table 11: One-side calculations

A-G fault	Impedance matrix	Negative Sequence	Saha One	Modified Saha
Kilometer	42	30	NA	64

Table 12: Two-side calculations

Chapter seven

Conclusions

The amount of transmission fault is growing and changing the network condition both in normal operation and during fault occurrences. The topic of this work involves intermittent and mechanical short circuit faults condition. There is an increased focus on reducing faults and calculate distance to fault to reducing the durations and cost for non-delivered energy. A more automated distance to fault calculation is considered to reduce outage times and research time of fault causes. Distance to fault calculation has different accuracy today depending of fault type and selection of algorithm. This thesis complies and evaluates different methods for classification of fault type and distance to fault. Different algorithms have been implemented, tested and verified to create a greater understanding of determinants facts that affect distance to faults algorithm's accuracy.

Distance to fault algorithm´s accuracy depends upon many different reasons and some algorithms are usually specified for a given type of fault, in design and structure related to occurring factor (fault resistance, zero-sequence system, ground system etc.) included in the analysis. Among analyzed technique, background information and evaluated algorithms is this problematic fundamental, especially when ground faults occur. In reality, the zero – sequence system will be varied towards different impedances and resistances to ground impact on verifying soil conditions.

Every implemented algorithm has been tested on the data generated from a number of simulations in Simulink for a verification process in implemented algorithms accuracy. In the verification process different fault cases have been tested and verified at different fault resistance. The effect on a higher fault resistance has negative affect on Modified takagi, Wisziewski and Novosel algorithm, when Harrysson and Takagi algorithms are more stable. This verification in accuracy depends on the algorithms reducing effect of load flow and effect of fault resistance with use pre-fault and fault data.

Two-terminal algorithms are capable to provide very accurate results if certain criteria are met, such availability of synchronization and data. Two-ended algorithms are capable of locating faults within or outside the mutually couple section if the right data is localized from the various line terminals. Verification process of algorithms Impedance matrix, Negative Sequence, Saha One, Modified Saha was carried out for a number of fault scenarios, same as used in one-side verification. Impedance matrix and Negative Sequence performed good fault margin accuracy at different simulated fault scenarios. Algorithm Saha One and Modified Saha were very unstable during the simulation, which is probably due to execution and data input on simulations solver function.

Fault estimation in chapter six presents an interesting comparison between the verification process and real fault location test in chapter seven. Accuracy of one-side algorithms is overall very high at different selected fault case. Based on calculations made in Simulink and the real test case, some algorithms have a certain fault margin. For real test cases the available data

quantity is more limited, but according to calculated results implemented one-ended algorithms overall presented a good fault location estimation.

For two-sided estimates the margin of fault is much greater, both in the validation process and at real fault case. This may depend on incorrect implementation of algorithms or lack of valid information. Two-side algorithm Negative Sequence method and Impedance matrix method provide better fault location estimation in the verification process than Saha One and Modified Saha for a transmission line model. On the contrary, all two-side algorithms present a high fault margin at real tested fault situation. Two-side methods provide fault location estimation with acceptable error. But in reality, two-sided algorithms are more accurate than one-sided algorithms, which may indicate a fault in the implementation or developed model.

The developed calculation model presented in chapter seven has been developed in collaboration with Enfo Consulting AS. The model presents an easily manageable collection of all implemented algorithms. The model has been developed in order to more easily compare implemented algorithms with each other and at various fault cases. A stochastic graph presents the results for distance calculations in a plot of distance to fault in kilometers.

Future work

A future implementation of the software and developed model in Statnett's network requires additional processing and validation of the algorithms' reliability and accuracy. Several more test cases need to be calculated and evaluated. Also several of the new solvers should be verified and tested further in the developed Simulink model.

Several two-sided algorithms should be implemented and verified in order to understand the methodology behind the fault handling and data verification. The extensive literature survey that underlies this thesis can be a good start for further development.

This report will form the basis for a comprehensive and important future work in meteorological aspects and impacts at the different fault situations on overhead. Performed calculations and information from test cases should be compared and implemented with the following metrological characteristics; Lightning (geographical point of impact), wind (direction) and temperature (icing, humidity).

Chapter eight

References

Books

[B.1.] M.M Saha. J.Izykowski, E.Rosolowski "Fault location on power networks" ISBN 978-1- 4471-2525-9

[B.2.] J. J.Izykowski " Fault location on power transmission lines" ISBN 978-83-7493-430-5

[B.3.] M. A. Salam ," Fundamentals of Power Systems" ISBN: 9781842655191

[B.4.] Grainger, John J. (2003). Power System Analysis. Tata McGraw-Hill. p. 380. ISBN 978-0-07-058515-7.

Papers

[1] *T.W Stringfield, D.J Marihart, " Fault location methods for overhead lines" Transactions of the AIEE, Part III, Power Apparatus and system, Vol 76, pp 518-530, Aug 1957*

[2] *J. Izykowski, R. Molag, E. Rosolowski, M. Saha, " A fault location method for application with current differential relays of three-terminal transformers"* IEEE Transactions on Power Delivery, Vol. 22,No 4, October 2007

[3] *P.K Dash, A.K Pradhan, G.Panda, A.C Liew, " Adaptive relay setting for flexible AC transmission system"* IEEE Transactions on Power Delivery, Vol. 15,No 1, January 2000

[4] *Anantachai Pongthavornsawad, Weerapun Rungseevijitprapa, "Broken Conductor Detection for Overhead Line Distribution System "*

[5] *G. Idarraga, Cubillos and L. Ibanez., "Analysis ofArcing Fault Models" , IEEE,*

[6] *J. Izykowski, R. Molag, M.Bozek, " Fault location on three terminal overhead lines with using two terminal synchorinized voltage and current phasors, International Symposium: Modern Electric Power System, September 2006.*

[7] *Korejwo, E . Synal, B " Short HV transmission line protection problems" IEE conf. Publ, 185,1980.*

[8] *Adly A. Girgis, David G. Hart, William L Peterson, " A new fault location technique for two – and three terminal lines", Transactions on Power Delivery, Vol 7, No7, January 1992.*

[9] *Majid Kermani, Masoud Farzaneh, Fellow, "The Effects of Wind Induced Conductor Motion on Accreted Atmospheric Ice" IEEE TRANSACTIONS ON POWER DELIVERY, VOL. 28, NO. 2, APRIL 2011*

[10] *May, H.S, "The design of overhead electric lines for improved reliability" , North Eastern Electr. Board, Newcastle upon Tyne, UK.*

[11] *G.H. Kjolle, O. Gjerde,T.Hjartsjo, H. Engen, L.Haarla, L.Kovisto, P.Lindblad, "Protection system faults a comperative review of fault statistics" KTH, Stockholm, Sweden –June 11-15, 2006*

[12] *Khalaf.Y.A " A new technique for location of fault location on transmission lines", Modern Applied Sciense, Vol 4, No:8 August 2010.*

[13] Damir Novosel. David G. Hart, Eric Udren, Jim Garitty "*Unsynchronized two-terminal fault location estimation"*, IEEE Transactions on Power Delivery, Vol. 11,No. 1, January 1996

[14] Karl Zimmerman, David Costello "Impedance based fault location experience", Schweitzer Engineering Laboratories, Inc. Pullman, WA USA.

[15] Hongling Sun, Vijay K. Sood, "*Impedance-based ground fault location for transmission lines*", UOIT, Oshawa, ON.

[16] A.Wiszniewski, "Accurate fault impedance location algorithm", IEEE *Transactions on Power Delivery, Vol. 130, No 6. , November 1983.*

[17] *A. Gopalakrishnan, M. Kezunovic, S. M. KcKennan, D. M. Hamai,"Fault Location Using the Distributed Parameter Transmission Line Model", IEEE Transactions on Power Delivery, Vol. 15, No. 4, October 2000.*

[18] *Dr. B.K Panigrahi, Dr. R. P. Maheshwari, "Transmission Line Fault Detection and Classification" PROCEEDINGS OF ICETECT 2011.*

[19] *Sukumar M. Brahma, Member, IEEE, and Adly A. Girgis, Fellow, IEEE "Fault Location on a Transmission Line Using Synchronized Voltage Measurements", IEEE TRANSACTIONS ON POWER DELIVERY, VOL. 19, NO. 4, OCTOBER 2004.*

[20] *Masayuki Abe and Nobuo Otsuzuki, Tokuo Emura and Masayasu Takeuchi "Development of a new location system for multi-terminal single transmission lines", IEEE Transactions on Power Delivery, Vol. 10, No. 1, January 1995.*

[21] *Adly A. Girgis David G. Hart William L. Peterson, "A new fault location technique for two - and three-terminal lines", Transactions on Power Delivery, Vol. 7 No.1, January 1992*

[22] *Joe-Air Jiang, Jun-Zhe Yang, Ying-Hong Lin, Chih-Wen Liu, Member, IEEE, and Jih-Chen Ma , "An Adaptive PMU Based Fault Detection/Location Technique For Transmission Lines", IEEE Transactions on Power Delivery, Vol. 15 No.2, January 2000.*

[23] *Song Guobing *, Suonan Jiale, Ge Yaozhong , "An accurate fault location algorithm for parallel transmission lines using one-terminal data", State Key Laboratory of Electrical Insulation and Power Equipment, School of Electrical Engineering, Xi'an Jiaotong University*

[24] *J. Izykowski, R. Molag, E. Rosolowski, M. Saha, "Accurate Location of Faults on Power Transmission Lines With Use of Two-End Unsynchronized Measurements", IEEE Transactions on Power Delivery, Vol.21, No.2, April 2006.*

[25] *T.Takagi, Y.Yamakoshi, M.Yamaura, R.Kondow, T.Matsuchima, "Development of a new type fault locator using the One-terminal and current data", IEEE Transactions on Power Apparatus and Systems, Vol. PAS-101, No. 8 August 1982.*

[26] *Jan Machowski, Janusz W. Bialek and James R. Bumby, Power System Dynamics- Stability and Control, 2nd Ed, John Wiley 2008*

[27] *A. Wiszniewski, "Accurate fault impedance locating algorithm", IEE PROCEEDINGS, Vol. 130, Pt. C, No. 6, NOVEMBER 1983.*

[28] *A.A Girgis, David G. Hart, William L. Peterson, "A NEW FAULT LOCATION TECHNIQUE FOR TWO- AND THREE-TERMINAL LINES", Transactions on Power Delivery, Vol. 7 No.1, January 1992.*

[29] *M.B. Djuric, Z.M. Radojevic and V.V. Terzija, "Distance protection and fault location utilizing only phase current data", IEEE Transactions on Power Delivery, Vol. 13, No. 4, October 1998.*

[30] *Leif Eriksson, M. Saha, G. D. Rockefeller "An accurate fault locator with compensation for apparent reactance in the fault resistance resulting from remote- End infeed." IEEE Power Engineering Review, February 1985.*

[31] *Carlos Eduardo de Morais Pereira, Luiz Cera Zanetta," Fault Location in Transmission Lines Using One-Terminal Postfault Voltage Data", IEEE TRANSACTIONS ON POWER DELIVERY, VOL. 19, NO. 2, APRIL 2004.*

[32] *M.B. Bjurib, Z.M. RadojeviC and V.V. Terzija, "Time domain solution of fault distance estimation and arcing fault detection on overhead line.", IEEE Transactions on Power Delivery, Vol. 14, No. 1, January 1999.*

[33] *R. Dutra, L.Fabiano, M.Saha, S. lidström. "Fault Location on Parallel Transmission Lines with Series Compensation", IEEE Transmission & Distribution Conference 2004.*

[34] Rastko Živanović, *"Evaluation of transmission line fault location techniques using variance-based sensitivity measured" The University of Adelaide, Australia*

[35] *C.F. Henville, "Digital Relay Reports Verify Power System Models", IEEE Transactions on Power Delivery, Vol. 13, No. 2, pp. 386-392, April 1998*

[36] *L.Eriksson, M.M Saha, G.D Rockefeller "An accurate fault locator with compensation for apparent reactance in the fault resistance resulting from remote-end infeed", IEEE Transactions on Power Delivery, Feb 1985*

Patent

[37] *Toshio Takagi, Yukinari Yamakoshi "Fault detecting system for locating a fault point with a fault resistance separately measured", United states patent PA:4313169, JAN 26,1982*

[38] *Damir Novosel , "Automatic fault location system" United States Patents PA:5455776, OCT 3,1995*

[39] *Damir Novosel, David Hart, Yi Hu, Jorma Myllymaki "System for locating faults and estimating fault resistance in distribution networks with tapped loads" United States Patent PA: 5839093, NOV 17, 1998*

[40] *M.M SAHA, "Method and device for locating a fault point on a three phase power transmission network". United States Patent PA:4559491, DEC 17, 1985*

Internet sources

[41] *Nordels statistics over fault in Scandinavia downloaded 14/5-2014.*
*"*http://www.fingrid.fi/fi/asiakkaat/asiakasliitteet/Kayttotoimikunta/2008/19.9.2008/nordel_fault_statistics_2007.pdf*"*

[42] *Symmetrical fault analysis 15/5 – 2014*
http://nptel.ac.in/courses/108107028/module4/lecture6/lecture6.pdf

Appendix A

Tutorial on Symmetrical Components

The use of symmetrical components is used to solve imbalanced problem with a balanced technique. This technique was developed by C.Fortescue 1917.

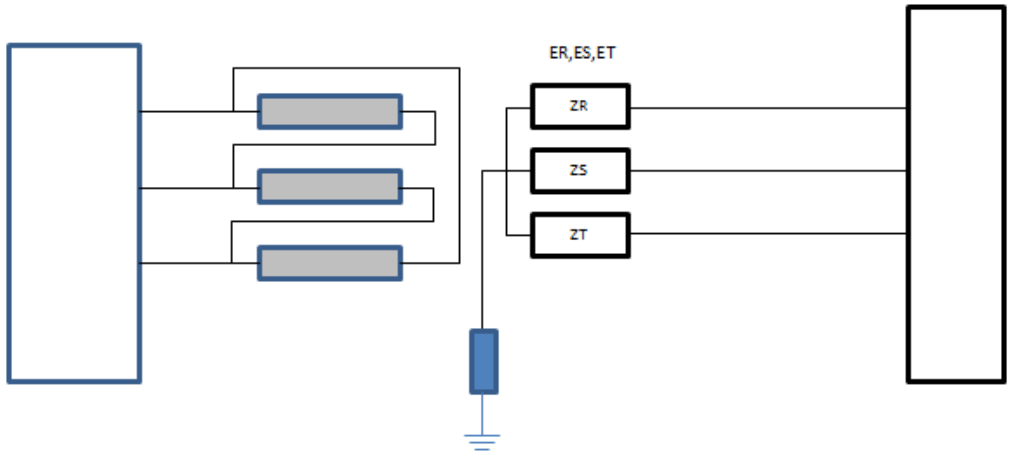

Figure 33: *Ungrounded power system*

The voltages over E_R, E_S, E_T in above figure can be described as:

$$\begin{cases} E_R &= U \\ E_S &= a^2 U \\ E_T &= aU \end{cases} \qquad a = -0{,}5 + j\frac{\sqrt{3}}{2} = <120°\,, \quad a^2 = -0{,}5 + j\frac{\sqrt{3}}{2} = <240°$$

Where (a) represents phase shift, voltages have equal amplitude and $120°$ phase shift. Following phase scheme when (E_R) is $120°$ before (E_S) and $240°$ before $(E_T)$is called *positive sequence* system. In a similar way, *negative sequence* are explained in the phase sequence when (E_R) are $120°$ after (E_S) and $240°$ after (E_T) and the *zero sequence* system explained where the phases have no phase shift to each other. The consequences are explained in the figure below:

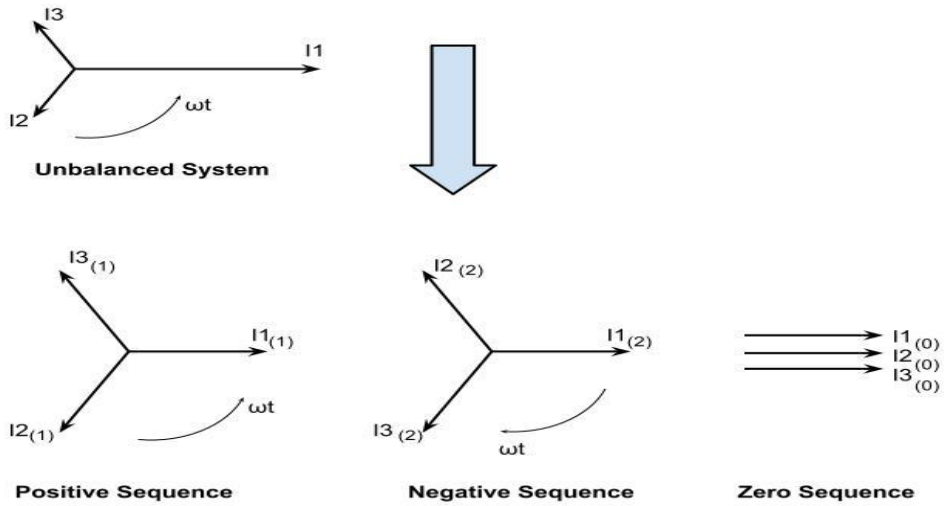

Figure 34 : Voltage represents in; Positive, Negative and Zero Sequence

$$\begin{cases} E_R = V = Ve^{j0} \\ E_S = a^2V = Ve^{j4\pi/3} \\ E_T = aV = Ve^{j2\pi/3} \end{cases} \qquad \begin{cases} E_R = V = Ve^{j0} \\ E_S = a^2V = Ve^{j2\pi/3} \\ E_T = aV = Ve^{j4\pi/3} \end{cases} \qquad \begin{cases} E_R = V = Ve^{j0} \\ E_S = a^2V = Ve^{j0} \\ E_T = aV = Ve^{j0} \end{cases}$$

Current sequences apply the same formula, but here the current phases are shifted to the phase voltage, which usually describes this respectively as (V_1) ,(V_2) , (V_3) for positive, negative and zero sequence. <- Titta på meningen ovan så att rättningen stammer överens med det du vill säga /gs. If following designations for phase voltage $(E_R), (E_S), (E_T)$ exchanged for (V_1) ,(V_2) , (V_3) this can be explained in a new matrix form:

$$\begin{bmatrix} V_R \\ V_S \\ V_T \end{bmatrix} = \frac{1}{3}\begin{bmatrix} 1 & 1 & 1 \\ 1 & a^2 & a \\ 1 & a & a^2 \end{bmatrix} * \begin{bmatrix} V_0 \\ V_1 \\ V_2 \end{bmatrix}$$

Were the first of the matrixes is phase voltage and the last matrix is sequence voltage.

Invers of the matrix equation:

$$\begin{bmatrix} V_0 \\ V_1 \\ V_2 \end{bmatrix} = \frac{1}{3}\begin{bmatrix} 1 & 1 & 1 \\ 1 & a & a^2 \\ 1 & a^2 & a \end{bmatrix} * \begin{bmatrix} V_R \\ V_S \\ V_T \end{bmatrix}$$

If above matrises are awarded in equation the following function is obtained:

$$V_0 = \frac{1}{3}(V_R + V_S + V_T)$$

$$V_1 = \frac{1}{3}(V_R + aV_S + a^2V_T)$$

$$V_1 = \frac{1}{3}(V_R + a^2 V_S + a V_T)$$

The first equation obtains zero sequence voltage as zero in a balanced system. This is becase of the sum of the three phase voltages is zero. Usually, lines are effected by asymmetri, which is due to induction, uneven loads etc. Unbalance in the system during a ground fault gives zero sequence components. This must be taken into consideration when calculating distance to fault.

Sequence current obtained corresponding to following formula:

$$I_0 = \frac{1}{3}(I_R + I_S + I_T)$$

$$I_1 = \frac{1}{3}(I_R + a I_S + a^2 I_T)$$

$$I_1 = \frac{1}{3}(I_R + a^2 I_S + a I_T)$$

which in matrix form can be written as:

$$\begin{bmatrix} I_0 \\ I_1 \\ I_2 \end{bmatrix} = \frac{1}{3}\begin{bmatrix} 1 & 1 & 1 \\ 1 & a & a^2 \\ 1 & a^2 & a \end{bmatrix} * \begin{bmatrix} I_R \\ I_S \\ I_T \end{bmatrix}$$

Transformer current in the neutral point is the sum of the phase current, which then gives:

$$I_N = I_R + I_S + I_T = 3I_0$$

If the system is balanced, will the zero current sequence componets be zeroe and this inverse current phaseobtained from:

$$\begin{bmatrix} I_R \\ I_S \\ I_T \end{bmatrix} = \frac{1}{3}\begin{bmatrix} 1 & 1 & 1 \\ 1 & a^2 & a \\ 1 & a & a^2 \end{bmatrix} * \begin{bmatrix} I_0 \\ I_1 \\ I_2 \end{bmatrix}$$

Appendix B

Verification of Simulink

Different types of fault are applied to the transmission line. The location of the fault is selected to 20 % of the total length and the fault resistance is chosen to $(0{,}1\ \Omega)$, $(5\ \Omega)$, $(10\ \Omega)$, $(30\ \Omega)$, $(50\ \Omega)$ to demonstrate the effect to the fault location estimation. The duration of fault is 0.9 seconds. The previous example shows the implementation of this in Simulink simulation. Fault location estimation for different fault with various fault resistance are presented.

Transmission line length	100 km
Distance to fault	20 %

A-G fault	Takagi	Modified takagi	Wisziewski	Novosel	Harrysson
$R_f = 0{,}1\ \Omega$	19,80 %	19,88%	20,22 %	20,07 %	19,95 %
$R_f = 5\ \Omega$	19,86 %	17,51 %	21,68 %	21,54 %	19,92 %
$R_f = 10\ \Omega$	19,66 %	15,32 %	22,29 %	22,93 %	19,84 %
$R_f = 30\ \Omega$	19,88 %	9,03 %	27,12 %	27,56 %	19,77 %
$R_f = 50\ \Omega$	19,90 %	5,75 %	30,97 %	33,26 %	30,9 %

A-G fault	Negative-Sequence	Saha One	Modified Saha	Impedance matrix
$R_f = 0{,}1\ \Omega$	19,35 %	28,02 %	42,06 %	21,32 %
$R_f = 5\ \Omega$	19,09 %	23,50 %	39,95 %	20,05 %
$R_f = 10\ \Omega$	18,02 %	24,22 %	42,44 %	19,52 %
$R_f = 30\ \Omega$	19,06 %	NA	NA	17,39 %
$R_f = 50\ \Omega$	15,55 %	NA	NA	16,25 %

B-C fault	Takagi	Modified takagi	Wisziewski	Novosel	Harrysson
$R_f = 0{,}1\ \Omega$	20 %	15,36 %	19,99 %	19,94 %	20 %
$R_f = 5\ \Omega$	19,76 %	NA	17,09 %	17,09 %	19,8 %
$R_f = 10\ \Omega$	19,40 %	NA	14,06 %	14,06 %	19,46 %
$R_f = 30\ \Omega$	18,88 %	NA	0,09 %	1%	18,88 %
$R_f = 50\ \Omega$	20,39 %	NA	NA	NA	20,39 %

B-C fault	Negative-Sequence	Saha One	Modified Saha	Impedance matrix
$R_f = 0{,}1\ \Omega$	23,80 %	31,40 %	22,48 %	20,10 %
$R_f = 5\ \Omega$	22,77 %	36,50 %	38,58 %	21,12 %
$R_f = 10\ \Omega$	22,22 %	NA	NA	21,70 %
$R_f = 30\ \Omega$	18,98 %	NA	NA	22,25 %
$R_f = 50\ \Omega$	15,90 %	NA	NA	22,68 %

A-B-G fault	Takagi	Modified takagi	Wisziewski	Novosel	Harrysson
$R_f = 0{,}1\ \Omega$	19,99 %	19,99 %	19,99 %	19,95 %	19,99 %

$R_f = 5\ \Omega$	19,76 %	16,16 %	17,09 %	17,09 %	19,75 %
$R_f = 10\ \Omega$	19,46 %	16,72 %	14,07 %	14,06 %	19,46 %
$R_f = 30\ \Omega$	18,88 %	NA	NA	NA	18,88 %
$R_f = 50\ \Omega$	20,39 %	NA	NA	NA	20,39 %

A-B-G fault	Negative-Sequence	Saha One	Modified Saha	Impedance matrix
$R_f = 0{,}1\ \Omega$	16,33 %	26,22 %	38,25 %	19,98 %
$R_f = 5\ \Omega$	15,88 %	39,88 %	32,83 %	21,63 %
$R_f = 10\ \Omega$	15,15 %	NA	39,8 %	21,75%
$R_f = 30\ \Omega$	11,65 %	NA	21,85	21,80 %
$R_f = 50\ \Omega$	18,45 %	NA	NA	21,86 %

A-B-C fault	Takagi	Modified takagi	Wisziewski	Novosel	Harrysson
$R_f = 0{,}1\ \Omega$	20,00 %	19,69 %	19,94 %	19,95 %	20,01 %
$R_f = 5\ \Omega$	19,76 %	NA	17,10 %	17,09 %	19,75 %
$R_f = 10\ \Omega$	19,47 %	NA	14,06 %	14,05 %	19,46 %
$R_f = 30\ \Omega$	18,85 %	NA	8,5 %	10,01 %	18,89 %
$R_f = 50\ \Omega$	20,40 %	NA	NA	NA	20,39 %

A-B-C fault	Negative-Sequence	Saha One	Modified Saha	Impedance matrix
$R_f = 0{,}1\ \Omega$	NA	NA	NA	19,99 %
$R_f = 5\ \Omega$	NA	NA	NA	20,00 %
$R_f = 10\ \Omega$	NA	NA	NA	20,10 %
$R_f = 30\ \Omega$	NA	NA	NA	20,50%
$R_f = 50\ \Omega$	NA	NA	NA	20,60 %

Appendix C

Fault location Algorithm in MATLAB

```
function
oneSidedCalculateDistance2Fault(tss,Znom,Phase)

time = tss(1).ts.dt*(1:length(tss(1).ts.data));

% Input from Simulink Simulation
ZL0 = Znom(1);
ZL1 = Znom(2);
k   = (ZL0/ZL1 - 1 )/3;
[U,I,~,Isym] = getThreePhaseSystemComponents(tss);

%One-Side Algorithm
%Initializing (IS) and (VS) at different fault

Is0 = Isym(:,3);

% Calculation of fault loop voltage and current at different fault situation

if length(Phase)==1
    IS = I(:,Phase);
    Is = IS+k.*3.*Is0;
    VS = U(:,Phase);
    if Phase == 1
        Isf1 = 1/3 * (IS + exp(1i*120*pi/180) * I(:,Phase+1) +
exp(1i*240*pi/180) * I(:,Phase+2));
    end
    if Phase == 2
        Isf1 = 1/3 * (IS + exp(1i*120*pi/180) * I(:,Phase+1) +
exp(1i*240*pi/180) * I(:,Phase-1));
    end
    if Phase == 3
        Isf1 = 1/3 * (IS + exp(1i*120*pi/180) * I(:,Phase-2) +
exp(1i*240*pi/180) * I(:,Phase-1));
    end
    I_sup = 3*(Isf1 - Isf1(1));
else
    IS = I(:,Phase(1)) - I(:,Phase(2));
    Is = IS;
    VS = U(:,Phase(1)) - U(:,Phase(2));
    I_sup = (I(:,Phase(1))-I(1,Phase(1))) - (I(:,Phase(2))-I(1,Phase(2)));
end

% Calculation of Pre-fault Current.
Is_pre = IS(1);
% Calculation of Superimposed Current Using Fault and Pre-fault Current.
I_mat =(IS-Is_pre);
% Calculation of Impedance.
Z = VS./Is;
%--------------------------------------------------------------------------
%Takagi Algorithm
dist2fault(:,1)= imag(VS.*conj(I_sup))./(imag(ZL1.*Is.*conj(I_sup)));
methodName{1}  = 'Takagi';

%--------------------------------------------------------------------------
```

```
%Modified Takagi -Zero Sequence Current Method with Angle Correction
[~,id] = max(abs(IS));
ang = angle(Is(id)./(3*Is0(id)));
dist2fault(:,2) =
imag(VS.*conj(Is0.*3).*exp(1i*ang))./imag(ZL1*Is.*conj(Is0.*3).*exp(1i*ang));
methodName{2}  = 'Modified takagi ';

%------------------------------------------------------------------------
%Wiszniewski Algorithm
ang = angle(ZL1);
a = real(I_sup./IS);
b = imag(I_sup./IS);
dist2fault(:,3) = imag(Z)./imag(ZL1) - ((real(Z)*tan(ang)/imag(ZL1) -
imag(Z))./imag(ZL1)....
    ./(a./b*tan(ang) - 1));
methodName{3}  = 'Wiszniewski';

%------------------------------------------------------------------------
%Novosel - Simple Reactanse Algorithm.
dist2fault(:,4) = imag(Z)./imag(ZL1);
methodName{4}  = 'Novosel';

function [time,data,ZLabc,tss] = alignTwoSidedMeasurements(tss1,tss2)

%data has the following components
%data(:,1:3) = three phase voltages S-side
%data(:,4:6) = three phase currents S-side
%data(:,7:9) = voltage symmetrical components S-side
%data(:,10:12) = current symmetrical components S-side
%data(:,13:15) = three phase voltages R-side
%data(:,16:18) = three phase currents R-side
%data(:,19:21) = voltage symmetrical components R-side
%data(:,22:24) = current symmetrical components R-side

%Side 1
dat(1).valid = tss1(1).ts.t0 +
tss1(1).ts.dt*(1:length(tss1(1).ts.data))/24/60/60;
t0(1) = tss1(1).ts.t0;
tTrig(1) = tss1(1).ts.trigger;
L(1) = length(tss1(1).ts.data);
dt(1) = tss1(1).ts.dt;

[dat(1).ts(:,1:3),dat(1).ts(:,4:6),dat(1).ts(:,7:9),dat(1).ts(:,10:12)] =
getThreePhaseSystemComponents(tss1);
p = calcPowerFromAnalogChannels(tss1);
smpl = datevec(tTrig(1)-t0)/tss1(1).ts.dt;
smpl = smpl(end);
prefaultMeanP(1) = mean(p(1:smpl/2));
clear p

%Side 2
dat(2).valid = tss2(1).ts.t0 +
tss2(1).ts.dt*(1:length(tss2(1).ts.data))/24/60/60;
t0(2) = tss2(1).ts.t0;
tTrig(2) = tss2(1).ts.trigger;
L(2) = length(tss2(1).ts.data);
dt(2) = tss2(1).ts.dt;

[dat(2).ts(:,1:3),dat(2).ts(:,4:6),dat(2).ts(:,7:9),dat(2).ts(:,10:12)] =
getThreePhaseSystemComponents(tss2);
p = calcPowerFromAnalogChannels(tss2);
smpl = datevec(tTrig(2)-t0)/tss2(1).ts.dt;
```

```
smpl = smpl(end);
prefaultMeanP(2) = mean(p(1:smpl/2));

%IDdir is the source station
[~,IDdir] = max(prefaultMeanP);

[~,ID] = min(L);
[~,IDn] = max(L);
new = interp1(dat(IDn).valid,dat(IDn).ts,dat(ID).valid);
time = dt(ID)*(1:length(new));
if ID==IDdir
    newData = [dat(ID).ts new];
else
    newData = [new dat(ID).ts];
end
data = newData;
id = sum(isnan(data)')>0;
id = id==0;
time = time(id);
data = data(id,:);
%get loop impedances matrix from S-side
eval(['tss = tss' num2str(ID) ';']);
ZLabc = getLoopImpedanceMatrix(tss);

eval(['tss = tss' num2str(ID) ';']);
% tss = tss1; %send back tss1 by default
for ii = 1:length(tss)
    try
        t = tss(ii).ts.dt*(1:length(tss(ii).ts.data));
        tss(ii).ts.data = interp1(t,tss(ii).ts.data,time);
    catch
    end
end

function dist2fault = NegativeSequenceTwoEnd(data,Znom)

% Input value
ZL2 = Znom(3);
VS2 = data(:,8);
IS2 = data(:,11);
VR2 = data(:,8+12);
IR2 = data(:,11+12);

ZS2 = VS2./IS2;
ZR2 = VR2./IR2;

% Negative sequence algorithm

a=real(IS2.*ZS2);
b=imag(IS2.*ZS2);
c=real(IS2.*ZL2);
d=imag(IS2.*ZL2);
e=real(ZL2+ZR2);
f=imag(ZL2+ZR2);
g=real(ZL2);
h=imag(ZL2);
A=abs(IR2).^2*(g.^2+h.^2)-(c.^2+d.^2);
B=-2*abs(IR2).*(e*g+f*h)-2*(a.*c+b.*d);
C=abs(IR2).^2.*(e.^2+f.^2)-(a.^2+b.^2);

for ii=1:length(A)
    P = [A(ii) B(ii) C(ii)];
```

```
    m = roots(P);
    D6(ii) = m(1);
    if length(m)>1
        for n=1:2
            if m(n)<=1 && m(n)>=0
                D6(ii) = m(n);
            end
        end
    end
end

dist2fault(1,:) = D6;

function dist2fault = to_sidig(data,ZLabc)

Vsabc = data(:,1:3);
Isabc = data(:,4:6);
Vrabc = data(:,13:15);
Irabc = data(:,16:18);

left = (Vsabc - Vrabc) + (Irabc*ZLabc);
right = (Isabc + Irabc)*ZLabc;

for ii = 1:length(data)
    Y = [real(left(ii,:)) imag(left(ii,:))]';
    D = [real(right(ii,:)) imag(right(ii,:))]';
    dist2fault(ii) = Y\D ;
end
dist2fault = abs(dist2fault);

function dist2fault = SahaAlgorithmPosSequence(data,Znom,Phase)

ZL0 = Znom(1);
ZL1 = Znom(2);
ZL2 = Znom(3);
k   = (ZL0-ZL1)/ (3.*ZL1);

IS1 = data(:,10);
IS2 = data(:,11);
IS0 = data(:,12);
VS1 = data(:,7);
VS2 = data(:,8);
VS0 = data(:,9);

if length(Phase)==1
    VS = data(:,Phase);
    IS = data(:,Phase+3);
    VR = data(:,Phase+12);
    IR = data(:,Phase+3+12);
    Is = IS1+k.*3.*IS0;
    if Phase == 1
        Isf1 = 1/3 * (IS + exp(1i*120*pi/180) * data(:,Phase+3+1) +
exp(1i*240*pi/180) * data(:,Phase+3+2));
    end
    if Phase == 2
        Isf1 = 1/3 * (IS + exp(1i*120*pi/180) * data(:,Phase+3+1) +
exp(1i*240*pi/180) * data(:,Phase+3-1));
    end
    if Phase == 3
        Isf1 = 1/3 * (IS + exp(1i*120*pi/180) * data(:,Phase+3-2) +
exp(1i*240*pi/180) * data(:,Phase+3-1));
    end
```

```
    I_sup = 3*(Isf1 - Isf1(1));
else
    VS = data(:,Phase(1)) - data(:,Phase(2));
    IS = data(:,Phase(1)+3) - data(:,Phase(2)+3);
    VR = data(:,Phase(1)+12) - data(:,Phase(2)+12);
    IR = data(:,Phase(1)+3+12) - data(:,Phase(2)+3+12);
    Is = IS;
    I_sup = (data(:,Phase(1)+3)-data(1,Phase(1)+3)) - (data(:,Phase(2)+3)-
data(1,Phase(2))+3);
end
Is_pre = IS1(1);

IR1 = data(:,10+12);
IR2 = data(:,11+12);
IR0 = data(:,12+12);
VR1 = data(:,7+12);
VR2 = data(:,8+12);
VR0 = data(:,9+12);

ZR1 = VR1./IR1;
ZR0 = VR0./IR0;
ZS1 = VS1./IS1;
ZS0 = VS0./IS0;
ZS2 = VS2./IS2;

K1  = (VS./(Is.*ZL1) + 1 + (ZR1./(ZL1)));
K2  = ((VS./(Is.*ZL1).*(ZR1./ZL1)) + 1);
%K3 = ((max(abs(Is)) - abs(Is(1))./(Is * ZL1)).*(((ZS1 + ZR1)./ZL1) + 1);
K3 = (I_sup./(Is * ZL1)).*(((ZS1 + ZR1)./ZL1) + 1);

A = ones(length(K1),1);
B = ((imag(K1).* real(K3)) - (real(K1).* imag(K3)))./(imag(K3));
C = ((real(K2).* imag(K3)) - (imag(K2).* real(K3)))./(imag(K3));

A0 = (ZL1.*VS./Is);
A1 = (ZL1 + ZR1) - (ZL1.*VS./Is);
A2 = -ZL1.*ZL1;
A00 = (ZS1+ZR1+ZL1).*I_sup./Is;

B0 = (real(A0).*imag(A00))-(imag(A0).*real(A00));
B1 = (real(A1).*imag(A00))-(imag(A1).*real(A00));
B2 = (real(A2).*imag(A00))-(imag(A2).*real(A00));

for ii = 1:length(A)
    m(1) = (-B(ii) + sqrt(B(ii)^2 - 4*C(ii)))/2;
    m(2) = (-B(ii) - sqrt(B(ii)^2 - 4*C(ii)))/2;
    mm(1) = (-B1(ii) - sqrt(B1(ii).^2 - 4*B2(ii).*B0(ii))./(2*B2(ii));
    mm(2) = (-B1(ii) + sqrt(B1(ii).^2 - 4*B2(ii).*B0(ii))./(2*B2(ii));
%     P = [A(ii) B(ii) C(ii)];
%     m = roots(P);
    D1(ii) = m(1);
    D2(ii) = mm(1);
    if length(m)>1
        for n=1:2
            if abs(m(n))<=1 && abs(m(n))>=0
                D1(ii) = m(n);
            end
        end
    end
    if length(mm)>1
        for n=1:2
            if abs(mm(n))<=1 && abs(mm(n))>=0
                D2(ii) = mm(n);
```

```
            end
        end
    end
end
dist2fault(:,1) = abs(D1);
dist2fault(:,2) = abs(D2);

% K1 = ZL1 - ZR1;
% K2 = -ZL1;
% K3 = ZS1 + ZR1 + ZL1;
% K4 = ZL2 - ZR0;
% K5 = -ZL0;
% K6 = ZL2 + ZS0 + ZR0;
%
% dist2fault(:,2) = (K1.*K3.*IS0)-
(K4.*K3.*(0*I_sup+1*IS2))./(K5.*K6.*(0*I_sup+1*IS2)) - (K2.*K3.*IS0);
% dist2fault(:,3) = ((VS1-VR1).*IR1-(VS2-VR2).*IR2)./(IS1.*IR2)-(IS2.*IR1);
```

Mattias is a young professional with over 3 years' experience in the industrial sector and 2 years' engineering experience in the energy sector, mainly related to R&D and Smart Grid projects in the Nordic countries (2014).

Mattias scientific interest involve: Sales Management,SmartGrids, Fault Management, Energy efficiency in buildings and industrial applications, Wind Designing, Land / Offshore WindPower, Nordic Regulation System, Project Management

LinkedIn: no.linkedin.com/pub/mattias-harrysson/58/b5a/64/

HALMSTAD UNIVERSITY

PO Box 823, SE-301 18 Halmstad
Phone: +35 46 16 71 00
E-mail: registrator@hh.se
www.hh.se